FINAL STUDY REPORT

SCEPTRON VIBRATION SPECTRUM SENSOR

IMPROVED SCEPTRON(TM)

SPERRY GYROSCOPE COMPANY
DIVISION OF SPERRY RAND CORPORATION
GREAT NECK, NEW YORK

Prepared for

G.C. MARSHALL SPACE FLIGHT CENTER

HUNTSVILLE, ALABAMA

CONTRACT NO.: NAS 8-2060

CONTRACT TITLE: 9-00-1-01100-302246 (Improved Sceptron)

PERIOD COVERED: June 6, 1966 to October 6, 1966

Doc. No.: HB-I.D.-9222-0243

TABLE OF CONTENTS

ILLUSTRATIONS

ILLUSTRATIONS (Continued)

SECTION I - INTRODUCTION

1.1 Scope of Report

This final report, covering the period 6 June 1966 through 6 October 1966, presents the results of a study concerning the design feasibility of a 100 Hz fiber optic device capable of measuring the frequency spectrum of a complex mechanical input forcing function. In the intended application, the device would be mounted on a structural member of a missile whose vibration spectrum is to be measured. The primary features of the fiber optic device are that it would be directly excited by the missile structure's vibration, and that the device's output is an optical analogue of the vibration spectrum.

The fiber optic device under consideration is basically a refinement of the vibrating reed frequency analyzer. Its operational principals are self evident from figures 1 and 2. Its outstanding features are very small size, high frequency resolution, wide frequency range, controlled reed (fiber) bandwidth an an optical readout of the reed amplitudes. The optical output consists of a sheet beam of light whose intensity versus distance measured from one edge of the sheet beam is an analogue to the vibration spectrum amplitude versus frequency.

The device is one of two types of vibrating fiber optic devices developed at Sperry for which the label SCEPTRON™ has been coined. The type of Sceptron under consideration here

consists of a row of metal reeds (fibers) whose frequency increases uniformly across the array. It was developed for use in a real time spectrum analyzer having a continuous printout on oscillographic recorder paper, but it should also find application in other systems which require a high quality and easily useable presentation of a signal spectrum. The other type of Sceptron developed at Sperry consists of a square array of vibrating glass fibers. It has been used in audio pattern recognition systems. It is not well suited to the present task and is not discussed in this report.

The Sceptron array developed for the spectrum analyzer covers a frequency range of 2 KHz to 6 KHz with 200 fibers each having 20 Hz bandwidth. Such an array was manufactured and enclosed in a special housing under Task I of this contract and delivered to the customer for evaluation. This report fulfills the requirements of Task II of this contract. It is a design study whose purpose is to derive the basic formula needed to extend the frequency range of the Sceptron array to .1 KHz to 20 KHz, and to determine the feasibility of such an extension of frequency range. Because a complete analysis has never been carried out previously on the standard 2 KHz to 6 KHz Sceptron array, in many instrances general formula had to be derived. These formulas were used to analyse the standard Sceptron as well as determine the basic design parameters of arrays to cover the extended frequency range.

1.2 Conclusions

A number of conclusions have been formed, a few favorable, most of them unfavorable, concerning the feasibility of covering the .1 KHz to 20 KHz frequency range. An overall yes-no type conclusion was not possible because too much depends upon the customer's specific requirements and the competitive approaches available to him, information not available to Sperry. The conclusions are as follows:

a. The design objective frequency range of 100 Hz to 20,000 Hz must be covered with four separate arrays covering the frequency ranges of 100 to 376 Hz, 376 to 1410 Hz, 1410 Hz to 5320 Hz, and 5320 Hz to 20,000 Hz. This is necessary in order to prevent higher mode excitation of the array fibers. A further requirement is that the arrays be mounted on mechanical filters which band limit the signal applied to each array to a frequency less than 6 times the lowest frequency of the array.

b. The manufacturing problems associated with the arrays increase in order of increasing frequency. The three lowest frequency arrays are considered practical to build, but the high frequency array by itself, may be impractical, although not impossible to build. All can be built with good frequency accuracy and bandwidth control.

c. The high frequency array requires the development of a part which will limit the fiber motion to a safe maximum value. This is necessary in order to prevent fatigue failure in the fibers when strong signals are inadvertently applied. The successful operation of a fiber limiter must be demonstrated experimentally before it is possible to guarantee delivery of arrays operating above 6 KHz.

d. The required critical alignment of the static masks limits the temperature range over which the arrays can be used to about -30 to 170 degrees F, based on calculations. These figures have not been varified experimentally and development work to improve the temperature range would probably be necessary.

e. Unless special precautions are taken, the steady state acceleration of the missile will cause the low frequency fibers to be displaced an unacceptable amount up to a frequency to about 850 Hz. The static displacement can not be distinguished from the displacement due to vibrations. Possibly acceptable solutions to this problem are outlined in the report.

f. The theoretical input dynamic ranges of the four arrays are 41 db, 41 db, 35 db, and 23 db in order of increasing frequency. This is a relatively small dynamic range

for a device which is used as a sensor. Because signal spectrums frequently encompass very large dynamic ranges, it is customary in spectrum analysis to compress the dynamic range before analysis by techniques such as pre-emphasis and automatic gain control. This is not possible in the intended application.

g. The array readout should be averaged at each frequency of interest over a period of 10 or more fiber time constants if the signal is basically random as it is thought to be. If the array is scanned, this implies that successive scans are averaged over a period of 10 or more time constants. There are other restrictions on the scanning speed (see Section 2.2.3) which require very rapid scanning, therefore, many scans must be averaged. The purpose of averaging is to obtain a stable estimate of the signal spectrum. Even with steady state discrete frequency signals, there is a need for smoothing the spectrums over time. It is thought that this requirement will increase equipment complexity a good deal.

1.3 Recommendations

It is recommended that the operating ranges, parameters, and limitations discussed in this report be carefully evaluated against missile operational conditions and requirements before broad band arrays are built. The high frequency array

should not be built unless it is absolutely necessary and it is determined that the additional development and manufacturing costs are worthwhile.

SECTION II - DETAILS OF DESIGN STUDY

2.1 General Discussion

This report discusses the factors involved in designing a metal fiber array which will frequency analyze the 100 to 20,000 Hz range. Several metal fiber arrays covering the 2000 to 6000 Hz range have been manufactured and tested previous to this program. Therefore the general nature of the problems to be encountered was known.

The essential parts of a metal fiber array of the type manufactured in Task I of this contract are shown in figure 1. This array covers the 2000-6000 Hz frequency range uniformly with 200 fibers in a 2 inch length. The fibers have a .002 x .022 inch cross section and vary in length from .098 inches to .170 inches. They have a 3 db bandwidth of 20 cps. The array is sandwiched between two photographic masks, also shown in figure 1. The operation of the array assembly is illustrated in figure 2. The array assembly is illuminated with collimated light. The fibers and masks block the light when the fibers are in their rest position. When the array assembly is attached to a vibration source, each fiber vibrates at its resonant frequency, f_o, with an amplitude proportional to the source spectrum amplitude at f_o. Thus the fiber amplitudes represent the source spectrum. The average light transmitted past each fiber is proportional to the

fiber amplitude, therefore the transmitted light intensity versus distance along the array represents the spectrum amplitude versus frequency.

A detailed analysis of array performance has been carried out in this report to accurately determine the design problems and the problems related to end use of the array. The performance analysis is broken down into the following categories:

2.2.1 Frequency range, number of fibers, fiber bandwidth as related to frequency resolution, transient response and stability of results.

2.2.2 Steady state transfer characteristics as function of fiber Q, light source collimation, diffraction and halation in photographic film.

2.2.3 Sources of noise with steady state signals, the need for smoothing.

2.2.4 Higher mode response of fibers. Frequency range that can be covered unambiguously with single array. Number of arrays required.

Following this, the practical design factors affecting performance are considered. These are:

2.3.1 Fiber stress. Its relation to frequency and dynamic range.

2.3.2 Dependence of bandwidth on air damping, fiber hysteresis, base hysteresis. Bandwidths obtainable.

2.3.3 Vibration levels needed to drive array.

2.3.4 Static displacement of fibers in array undergoing d.c. acceleration.

2.3.5 Magnetic coupling between fibers. Effect on design of low frequency fibers.

2.3.6 Critical dimensions. Thermal expansion problems. Tuning Accuracy.

2.3.7 Structural resonances.

Within each section, reference is made to the array delivered in Task I and to the 100 Hz to 20,000 Hz array whenever significant conclusions can be drawn or design information stated.

2.2 Performance Analysis of Array

2.2.1 Frequency Range, Number of Fibers, Fiber Bandwidth.

The frequency range to be analyzed is 100 to 20,000 Hz. An ideal analysis would obtain the signal spectrum[1] for all frequencies in this range. However, the metal fiber array consists of a set of fixed narrow band filters, so the array

---

1. The word "spectrum" is used loosely except where specifically defined. It is generally taken as meaning the amplitude response of a set of contiguous filters or, almost equivalently, the amplitude of the fourier transform of a weighted time segment of the signal.

output measures the signal spectrum as a set of discrete frequencies. If the fibers are close enough together, and if the fiber bandwidth is small enough, the spectrum fine structure will be adequately represented. It might seem from this statement that an ideal analyzer would have an infinite number of filters each having zero bandwidth, and this is true for ideal steady state discrete frequency signals. In general, however, the signals are changing with time, or the signals are random in nature. In the first case, if the changes are slow with time, the signal will be termed quasi-steady state, and interest naturally focuses on the signal spectrum measured over finite segments of the signal. Such a spectrum can be obtained by a set of contiguous filters having an impulse response whose duration matches the length of the signal segments. Such a bank of filters will have bandwidths of roughly one over the signal segment length because of the inverse relationship between bandwidth and duration of impulse response.

In the second case the signals are random, that is, noise-like. A model for such signals is a white noise generator driving a linear system. The output of the linear system will be noise, colored by the frequency response of the linear system. The amplitude frequency response of the linear system can be determined by means of a set of contiguous filters as in case one. However, in case two, it is necessary

to smooth the rectified output of each filter over 10 or more filter time constants to obtain a stable (reliable) estimate of the linear system's transfer function. The need for smoothing arises out of the random nature of the signal. The instantaneous filter output amplitude can range theoretically from zero to infinity when driven by a noise generator. It is the average output that is significant. The averaging time must be long enough, ten or more filter time constants, to obtain a good estimate of the long term average output. Therefore, if it is necessary to obtain a stable estimate quickly, broadband filters (having an impulse response whose duration is short) must be used. It is clear from above that there is a conflict between obtaining stable estimates quickly and good frequency resolution. If the linear system function is time dependent, a situation similar to case one developes. For a quasi stationary random signal, the signal can be divided into segments each of which is taken to be stationary. However, unlike case one, the filter response time must be a small fraction, one tenth or less, of the segment length. Therefore, the frequency resolution obtained is one tenth or less that obtained for case one. As a final remark, the signal analyzed always have a beginning and end, therefore the quasi stationary segment cannot be any longer than the signal duration. It can occur that the signal duration is

not great enough to obtain the desired stability and frequency resolution[2].

The conclusion to be drawn from the above discussion is that for each signal to be analyzed, a bandwidth should be chosen meeting both the resolution requirements and response time requirements. This is not always possible. With regard to this program Sperry does not know what the nature of the signals to be analyzed is except that they are probably noise-like. Furthermore, the range of bandwidths obtainable by means of vibrating fibers is rather small at present say 5 to 40 Hz over the 100 to 6000 Hz range. In general, several analyses with different bandwidths may be necessary to capture parts of the signal spectrum. Certainly, in the initial stages of signal analysis, several bandwidths should be tried to see which gives the best results.

The optimum fiber spacing is a function of the fiber bandwidth. The basic consideration is that the fiber spacing should be small enough so that the signal spectrum can be recreated accurately from the discrete samples provided by the array. In the following paragraphs, a near optimum method of recreating the signal spectrum will be presented. Several worst case signals will be used as examples. From these examples, the optimum fiber spacing versus bandwidth will be determined. The problem of recreating the signal spectrum is

---

2. The concepts of this paragraph are taken largely from R.B. Blackman and J.W. Tukey, "The Measurement of Power Spectra," Dover 1959.

essentially one of interpolating between the sample values. There are several ways of doing this physically. One way is to scan the array with a detector having a width equal to or greater than the fiber spacing. This operation is mathematically equivalent to convolving the sample data with a pulse of finite width. Another way is to diffuse the light output of the array, that is allow the light output of each fiber to spread slightly so that the region between fibers is filled in with light. This operation is also equivalent to convolution of the array output with a pulse. A third way is to scan the array output with a small detector and low pass filter the detector output. This is equivalent to convolving the array output with a pulse whose shape is the impulse response of the filter running backwards. A fourth and more esoteric way is to spatially filter the array output with a coherent optical processor. Of these, the first three are practical, the fourth is unnecessarily complicated.

The first and second techniques are illustrated in figure 3. In the former, a scanner moves across the array. The light sensitive surface gathers the outputs of several fibers, weights them by the amount indicated by the weighting function shown and sums them. In the latter technique, the output of each fiber strikes a diffuser. Each pencil of light spreads out and illuminates the photosensitive surface with an intensity versus position indicated by the weighting functions

drawn in. The photosensitive surface sums the distributions produced by each fiber. The two techniques give identical output versus position (within a constant factor) when the weighting functions are identical. Both techniques will be called spatial smoothing. The mathematical model that follows is based upon the second technique, but also applies to the first.

The light intensity versus position on the photosensitive surface is given by

$$L(f) = K\int_{-\infty}^{+\infty} D(\lambda) L_o(f-\lambda)\, d\lambda \qquad (1)$$

where f is distance along the photosensitive surface measured in terms of the resonant frequency of the fiber opposite the surface.

$L_o(f)$ is the light output of the array versus f.

$D(f)$ is the weighting function which results from the diffuser.

$L(f)$ is the light intensity incident on the photosensitive surface versus distance.

k is a constant dependent on transmission losses, which will be set equal to 1.

Conceptually, the action of the diffuser can be thought of as spatial filtering. To point this out, the Fourier transform of $L(f)$ is written below.

$$S(\xi) = \int_{-\infty}^{+\infty} L(f)\, e^{-j2\pi \xi f}\, df = Q(\xi) \cdot S_o(\xi) \qquad (2)$$

where ξ is the transform variable

$$S(\xi) \leftrightarrow L(f)$$
$$S_o(\xi) \leftrightarrow L_o(f)$$
$$Q(\xi) \leftrightarrow D(f)$$

The light output of the array can be approximated as the product of a sampling function and the continuous output that would have been obtained if the fiber spacing were infinitesimal. Thus

$$L_o(f) = \Delta f \sum_{n=-\infty}^{+\infty} \delta(f - n\Delta f) \cdot L_\infty(f) \qquad (3)$$

where Δf is the fiber spacing.

$\delta(f)$ is a dirac delta function.

$L_\infty(f)$ is the continuous output that would be obtained with infinitesimal Δf.

The transform $S_o(f)$ of $L_o(f)$ is found to be

$$S_o(\xi) = \sum_{n=-\infty}^{+\infty} S_{oo}\left(\xi - \frac{n}{\Delta f}\right) \qquad (4)$$

where $S_{oo}(\xi) \leftrightarrow L_\infty(f)$

Substituting (4) into (2), the final expression for $S(\xi)$ is obtained:

$$S(\xi) = Q(\xi) \cdot \sum_{n=-\infty}^{+\infty} S_\infty\left(\xi - \frac{n}{\Delta f}\right)$$

The nature of these functions is illustrated in figure 4. The action of the diffuser, in this example, is to remove higher sidebands from $S_o(\xi)$, leaving $S(\xi)$, which approximates the transform of the hypothetical continuous output that would be obtained if the fiber spacing were infinitesimal. Therefore, the light output, $L(f)$, is a good representation of this hypothetical output. Of course, if the fiber spacing is too large, the terms of $S_o(\xi)$ overlap so that $S_\infty(\xi)$ cannot be recovered accurately. Or if the weighting function, $D(f)$, is too wide, $Q(\xi)$ will be too narrow, and $S_o(\xi)$ will be truncated by $Q(\xi)$.

Perhaps the easiest way of analyzing the diffuser (or scanner) is to assume a weighting function and evaluate equation 1 for several input signals and fiber spacings. The weighting function that will be used is given by

$$D(f) = \frac{1}{2}\left(1 + \cos\frac{\pi f}{F}\right), \quad -F < f < F$$
$$= 0, \quad |f| > F \qquad (6)$$

This weighting function, called a hanning window, and its transform $Q(\xi)$, are sketched in figure 4. This window is chosen for the following reasons: it is a smooth curve which produces no discontinuities in magnitude or slope of the smoothed data. It is the general type of weighting function that one would expect a diffuser to produce. It is a simple mathematical expression and its transform has low sidelobes.

The first example of equation 1 is the smoothed output of a train of equal impulses equally spaced Δf. The peak to valley ratio of the smoothed output versus window width is shown in figure 5a. As shown, the peak to valley ratio is near one for $F > \Delta f$ and is one for certain values of window width. The second example consists of the smoothed output of the array when the input is a single frequency, the fiber has a square law detector transfer characteristic, the fibers are spaced one bandwidth apart and the window is three fiber spacings wide (figure 5b). Two cases are shown; when the input frequency coincides with a fiber and when the input frequency falls midway between two fibers. Fiber positions are indicated by circles. The dashed curves represent the array output assuming infinitesimal fiber spacing. The third example (figure 5c) is the same as the second except that the fiber spacing is one-half the bandwidth. This set of conditions was used in plotting figure 4 also (spatial filtering). In the fourth example (figure 6a), the fiber has a linear full-wave detector characteristic, the fibers are spaced one bandwidth apart and the window is three fiber spacings wide. The fifth example (figure 6b) is the same as the fourth except the fibers are spaced one-half bandwidth apart. In the sixth example (figure 6c) the fiber has a linear full-wave detector characteristic, the fibers are spaced one bandwidth apart, the window is three fiber spac-

ings wide, but the input is two equal amplitude frequencies three bandwidths apart. The seventh example (figure 7a) is the same except that the fiber spacing is one-half bandwidth and the input frequencies are spaced 1.5 bandwidths. The last example (figure 7b) is the same except the two input frequencies are one bandwidth apart.

These examples show that the smoothing technique employed works rather well when the fibers are spaced one-half bandwidth. Particularly, it should be noted that the peak values of the smoothed curves are nearly independent of the positions of the fibers relative to the curves. Also two frequencies 1.5 bandwidths apart can be resolved. Frequencies spaced one bandwidth apart cannot be resolved for the choice of fiber positions in figure 7b. This figure is of interest because it shows that an ideal array (infinitesimal fiber spacing) would just resolve frequencies one bandwidth apart. To maintain this resolution in a practical array would require that the fibers be spaced roughly one-third bandwidth apart (the spacing must be somewhat smaller than the separation of mins, and maxes, according to the sampling theorem). When the fiber spacing is one bandwidth, the array performance deteriorates considerably. The peak values depend to a greater extent on the relative positions of the fibers on the curves. More seriously, the array resolution is three bandwidths rather than the 1.5 bandwidths obtained with the smaller

fiber spacing. The decrease in resolution can be thought of as an increase in the effective bandwidth of the fibers, and is tolerable in some applications. Unfortunately, the response time is not reduced by the broadening effect smoothing has on the array output.

No further analysis of fiber spacing and smoothing is really necessary, however, it might be asked whether there is a better type of spatial filtering in terms of minimizing the number of fibers required for the same accuracy and resolution. An ideal low pass filter minimizes rms error, but has a undesirable ringing impulse response. Smoothing using a hanning window degrades the resolution by no more than a factor of about 1.5 (see above examples) from that which a loose application of the sampling theorem predicts as a limit. This is typical of practical systems.

The delivered array (2 KHz to 6 KHz has 20 Hz bandwidth fibers spaced 20 Hz apart, as do all arrays that have been manufactured to date. The above analysis shows that these arrays would have better performance if the bandwidths were increased to 40 Hz. This can be done by changing the amount of aerodynamic damping on the fibers. However, if the bandwidth is increased, a larger input vibration level is required, which could be a problem in some applications. The other alternative is to reduce the fiber spacing in the future. This is possible but expensive because of the high cost of manufacturing array fibers. Also the increased size

would in some cases be a problem. Each alternative must be considered in relation to the intended application. When the signals have no narrow peaks or valleys, as is often the case for noise like signals, then the above resolution and accuracy problems do not exist. However, even then it is highly desirable that the ability of the array to resolve narrow peaks not be sacrificed because the exact nature of the signals is after all unknown in most cases before the spectral analysis.

It was stated, in the discussion of spatial smoothing, that scanner and diffuser can have identical effects. This is true only as it applies to a completely fixed array output. Obviously, if the signal is changing, then the scanner will not see the same signal as the diffuser because of the finite scan rate. The problem presented by a noise signal is severe. On the one hand scanning should be rapid so as to see changes in the noise spectrum. On the other, the array output should be averaged over 10 or more time constants to permit the average spectrum at each frequency to be obtained with good accuracy. Using a hanning window 3 fiber spacings wide and a fiber spacing equal to the fiber bandwidth, B, the latter requirement is satisfied if the scan rate is less than $1/2\ B^2$ Hz/sec. This expression is obtained by dividing the mean window width by 10x (time constant). If the bandwidth is 20 Hz, the scan rate should be less than 200 Hz/sec, a very low rate of scan.

If the scan rate is violated seriously, it is necessary to record each scan and average enough scans (over a period of 10 or more time constants) to obtain stable results. The latter technqiue is preferrable in that changes in the spectrum will be perceived as well as they can be for the averaging time employed.

2.2.2 Steady State Transfer Characteristics

The steady state transfer characteristics of the array can be treated in two parts. The first part consists of determining the fiber motion when the signal is of the discrete frequency type. The second part consists of determining the light output as a function of fiber displacement. This function is nonlinear because of the effects of imperfect light collimation, clipping, diffraction, and halation in the photofraphic film used to make the static masks. The first step is to calculate the response of a fiber to a sinusoidal signal. This is done by means of the spring-mass-damper model of the fiber shown in figure 8. In this figure, y_1 represents the input displacement applied to the base of the array and y_2 represents the displacement of the fiber tip relative to the static mask. The model is accurate provided the fiber Q is high enough (greater than 10). The transfer function relating y_1 and y_2 is also given in this figure. It is seen that at resonance the output displacement is Q times the input displacement. The fiber behaves as a simple tuned circuit.

The light output as a function of fiber displacement depends upon the degree of light source collimation as well as diffraction and halation effects. These effects will be treated one at a time. Initially it is assumed that diffraction and halation are nonexistent, but that the source is a large lambertian source. This is illustrated in figure 9. As shown, some light can leak through the array even when the fibers are in their rest position. When a fiber is displaced, it allows a pencil of light to pass straight through the array, blocks the leakage path on one side and increases the leakage path on the other side. The relative magnitudes of these light fluxes are easily calculated. The entrance slits on the left side of the array are considered as line sources. The intensity of these sources is proportional to the angles they subtend at the various exit slits on the right side. These angles are shown with dashed lines. The light flux which emerges from the exit slits is proportional to the source intensity times the area of the emergent beam which in turn is proportional to the angle subtended by the exit slit as viewed from the entrance slit. Normalizing with respect to path 3, the relative fluxes are .25, .71 and 1 respectively for paths 1, 2 and 3. If the lower fiber is displaced one full fiber width, these numbers become .062, .35 and 1 normalized again with respect to path 3. The flux in path 3 is proportional to the square of the fiber displacement because it is proportion both to the area of the entrance slit and exit slit.

A more realistic drawing of the array is shown in figure 10. Here the fibers are shown slanted 5 degrees. Now the leakage components are much larger. When the bottom fiber is displaced one fiber width, the relative fluxes for paths 1, 2 and 3 are .72, .15, and 1 respectively. The light flux through path 3 is given by

$$L \simeq \frac{I_o \ell}{2w} y(y+a), \quad y \leq d-a$$

$$L \simeq \frac{I_o \ell d}{2w} y, \quad d-a \leq y < d \qquad (7)$$

where y is the fiber displacement.

a is a measure of the fiber slant (see figure 11).

w is the spacing between the masks.

I_o is the incident light intensity on the array.

ℓ is the length of fiber illuminated.

L is in lumens when the dimensions are in meters.

d is slit width.

The formula is accurate for $\ell \gg w$, is accurate enough for rough calculation down to $\ell = w$. For small fiber slant ($a \sim 0$), the transfer function is square law.

From the above analysis it is concluded that large lambertian sources cannot be used. In fact, the collimation must be good enough to exclude the possiblity of flux paths such as 1 and 2. A path such as 4 is also possible, because of the high reflectivity of the fibers. To exclude all of these leakage paths the source semi angle must be less than 9 degrees, for the dimensions shown in figure 10 (representative of arrays manufactured to date).

As shown above a large lambertion light source cannot be used. The small source semiangle can be most efficiently obtained by the use of a small source which either approximates a point source or a line source. A collimating lens must be used to render the light approximately parallel. A practical light source is shown in figure 11. It consists of a coil filament whose length runs parallel to the array fibers, a collimating lens, and a cylinder lens to form an intense line image of the source at the array.

The angle subtended by the source in the horizontal plane equals the source width divided by the distance between the source and the collimating lens. This included angle must be less than 18 degrees as explained above. However, there is no benefit to be gained by making the source angle greater than 10 degrees because this is the acceptance angle of the array when the static mask slots are fully exposed for the type arrays manufactured to date (see figure 11, bottom). With such a source, the light flux is proportional to the square of displacement for fibers having zero slant, as is the case for the large lambertion source. If the source is smaller than 10 degrees, the array transfer function will be square law up to a fiber displacement such that the array acceptance angle equals twice the source angle, and then will become linear. The transfer function is given by

$$L = \frac{I_o \ell}{2w\theta} y^2, \quad y \leq w\theta$$

$$L = I_o \ell \left(y - \frac{w\theta}{2}\right), \quad w\theta \leq y < d$$

(8)

where L is the light flux in lumens when dimenstions are in meters.

I_o is the intensity of illumination on the array.

ℓ is the length of fiber illuminated.

w is the separation between masks.

y is the fiber displacement.

θ is the included angle subtended by the source at the plane of the collimating lens.

The width of the line image incident upon the array equals the coil filament length multiplied by the ratio of the focal lengths of the cylinder lens to the collimator lens. This width is not critical. However, if it exceeds the width which the array assembly will accept, the design is not optimum in the sense that a smaller (lower power) source could have been used, or a shorter focal length lens could be used to put more light through the array. The delivered array, which is considered typical, will accept an included angle of 20 degrees and a line width of about .030 inches.

It is possible to obtain very small light sources such as fine filaments, zirconium arc lamps and high pressure mercury arc lamps. In this case, the array output will be approximately linear (except for the small effects of source size, diffraction

and halation). With a square law response, the array output represents the power spectrum, whereas with a linear response, the array output represents the amplitude spectrum. The power spectrum is easier to analyze analytically but otherwise has little advantage. It is to be noted that the effect of variations in fiber slant is less if a small source is used. For this reason small sources are favored.

Representative transfer functions are shown for the various cases discussed above in figure 12. The effect of clipping is indicated in each curve at a displacement equal to the mask slot width. An accurate curve showing the effects of clipping is also shown in figure 12, assuming a very small source. Unlike the other curves of figure 12, which are instantaneous light output versus instantaneous fiber position plots, the clipping curve is a plot of average light output over a cycle versus the peak amplitude of vibration. Because of clipping, fiber amplitudes greater than the slot width give little information about the spectrum amplitude.

In studying these curves an important factor to consider is dynamic range. Input dynamic range is the ratio of the maximum to minimum input for which the output is meaningful. Clearly the square law region in the transfer characteristic should either cover the entire range or be made very small. The former requires the use of a relatively large light source and the latter a very small one. Since fiber slant is not well

controlled at present, only a very small source gives a transfer characteristic which is mathematically simple and repeatable from fiber to fiber.

Diffraction has a pronounced effect on the dynamic range of the array, and is the most fundamental phenomenon limiting dynamic range. This effect owes its existence to the wave nature of light, and is important in the present case because the dimensions involved are not large compared to the wavelength of light. For instance, if a dynamic range of 40 db is desired and the fiber is .002 inches thick, a fiber displacement of 20 microinches must be detected, which happens to be one wavelength of green light.

Unfortunately, the diffraction effect is very difficult to analyze exactly and, therefore, it has been necessary to idealize the array geometry. Four models are presented and analyzed. All of them use specifically the basic dimensions of the array delivered in Task I (fiber cross section of .002 x .022 inches, mask to fiber clearance of .0015 inches), but the results are easily generalized by means of the scaling laws presented. The last model is particularly important because it shows how to extend the dynamic range and because it is fairly realistic for the delivered array. The first three models are used primarily to point out the basic problems.

Model number 1 is shown in figure 13. It consists of a single mask and a fiber which has two knife edges. The mask

is illuminated by a collimated light source. The intensity pattern incident upon the fiber can be calculated by means of Fresnel integrals[3] for each wavelength of incident light. To simplify the computation, a monochromatic source of wavelength .5 microns (green) is assumed. The intensity pattern is shown in figure 13 also. It should be noted that the intensity at the edge of the geometric shadow is only 1/4 that predicted by geometric optics. Also there is light in the shadow region.

To evaluate the instantaneous optical transfer function (light flux output versus fiber instantaneous displacement) the part of the intensity curve falling beyond the fiber edges is integrated for various fiber displacements. This curve is plotted in figure 14. Since the fiber motion is always approximately sinusoidal, the transfer function of interest is really the average light output over a cycle, versus the fiber peak amplitude. This is calculated by determining the shape of the light output pulses for several fiber amplitudes, then finding the area of these pulses. This transfer function is shown in figure 15. It is seen that light leaks through the array even when the fiber displacement is zero. This leakage component is about 1.7 percent of the light transmitted through the static mask slot. The light output does not increase significantly until the fiber displacement reaches $.07 \times 10^{-3}$ inches, or 70 microinches.

---

3. F.A. Jenkins, H.E. White "Fundamentals of Optics, " McGraw-Hill, 1950, p365-372.

The dynamic range can be determined from this curve. The definition of dynamic range is somewhat arbitrary, however, the general idea is that it should be a measure of the ratio of the maximum to minimum input signal levels for which the array gives useful outputs. The maximum fiber displacement that gives a useful output is one fiber thickness (2×10^{-3} inches in the example), because clipping occurs for larger displacements. The minimum useful displacement is about $.07 \times 10^{-3}$ inches. Therefore, the dynamic range is about 29 db.

The dynamic range is a function of mask to fiber clearance for model number 1. 3 db is added for each factor of two reduction in clearance. This scaling law is based upon the shape of the intensity curve (figure 13) as a function of mask clearance. This curve is scaled by the square root of clearance along the S coordinate. Dynamic range is also a function of fiber thickness. 6 db is added for each doubling of fiber thickness.

The dynamic range of the double mask arrangement of figure 9 (with small source) can be estimated more closely from model number 2 shown in figure 16a. In this case the diffraction pattern formed by the mask slit falls upon the far edges of the fiber. The left side mask is removed to make the analysis possible by means of Fresnel integrals as before (otherwise the calculation is too difficult to perform). Using the fact that 3 db of dynamic range is lost for each doubling of the spacing

between the first and second set of knife edges blocking the light, it is calculated that 12 db is lost. Therefore the dynamic range is 17 db.

If the fibers slant, then a possible model for diffraction effects is model number 3 shown in 16b. The analysis is essentially the same as for 16a, except now the fiber exposes a wider slot at full amplitude. For the delivered array, a 5 degree slant doubles the slot width hence 6 db is added to the dynamic range. The dynamic range becomes 23 db. A much larger slant cannot be used because rays could then be reflected off the fibers through adjacent slots (see figure 10).

As a result of the above analysis, a double mask arrangement having much more dynamic range was thought of. It is model number 4 shown in figure 17. The essential features of this arrangement are that the light rays make a non-zero angle with respect to the fibers, and that the mask slots be wider than the shadow cast by the fiber. One mask lines up with one corner of the fiber and the other mask lines up with the diagonally opposite corner of the fiber.

Consider the middle fiber in the drawing. In region 1, the mask straight edge causes a Fresnel diffraction pattern to fall upon the first edge of the fiber. This is the situation treated in figure 13, so at this location, the minimum preceptible fiber displacement is about 70 microinches. However, what counts is the light which passes through the slit in region 2. This slit

is large, therefore, it can accommodate the wide diffraction pattern that slit 1 forms when the fiber displacement is small. The shape of this pattern is calculated approximately by assuming that slit 1 is uniformly illuminated as predicted by geometric optics, and then calculating the diffraction pattern formed at slit 2 by slit 1. For very small displacements, Fresnel diffraction can be approximated by Fraunhofer diffraction, hence the width of the main lobe will be[4]

$$d = \frac{2w\lambda}{y}$$

where d is the width of the main lobe.

w is the width of the array.

λ is the wavelength.

y is the fiber displacement.

For a 70 microinch displacement, d is .0125 inches whereas slit 2 is .004 inches wide, hence only one third of the main lobe is accommodated. However, this center third contains two thirds of the light in the diffraction pattern, so it is concluded that slit 2 does not noticeably degrade the dynamic range.

Slit 3 is also wide. It causes a Fresnel diffraction pattern to fall upon region 4. However, the fiber is reflective so it is also possible to have interference between the direct

---

4. Ibid 3, pp 279-285

and reflected rays reaching region 4. First consider diffraction. The straight edge diffraction pattern shown in figure 13 can be used. Because the distance of the knife edge is 16 times as great as in figure 13, the distance, S, to the first maximum is 4 times as great, or .0006 inches. The actual distance, S, is .002 inches, so diffraction can be neglected to the first approximation.

Interference arises between the direct and reflected ray as shown in figure 18. The maxima are separated by a distance equal to 115 microinches for an angle θ equal 5 degrees. If the fiber surface acts as perfect metal reflector, then the first node is at the corner of the fiber when the incident light is polarized perpendicular to the plane of incidence, and the first maxima is at the corner when the incident light is polarized in the plane of incidence. Therefore, when the source is randomly polarized, no net interference pattern should be visible. Nevertheless, such a pattern was observed microscopically when the delivered array was being assembled. The pattern disappeared when the angle θ was made about 5 degrees, but is very apparent for small angles. Possibly the fiber surface partially polarizes the light or possibly the first edge of the fiber tends to reflect the component perpendicular to the plane of incidence when the angle θ is small. At any rate, for angles greater or equal to 5 degrees, the slit labeled 4 is by observation, quite uniformly illuminated.

and, therefore, the model 1 analysis can be applied, yielding a minimum observable displacement of 70 microinches.

Since the fiber maximum useful displacement is .004 inches and the minimum useful displacement is 70 microinches, the dynamic range is 57 to 1, or 35 db, using green light (.5 microns). If silicon detectors and tungsten filament sources are used, a more realistic wavelength to use is .7 microns. Based on the fact that straight edge Fresnel diffraction pattern scales as the square root of wavelength, the dynamic range is reduced by a factor 1.2, or 1.5 db.

With model 4, the source should be small enough so that the penumbra width at the edge of the fiber labeled 1 is considerably less than 70 microinches, say 30 microinches. This condition is satisfied if the source subtends less than 2 degrees at the collimator. For similar reasons the array should be aligned within 1 degree.

Model 4 (figure 17) shows the fibers perpendicular to the array masks. In actual practice, the fibers are only approximately perpendicular. The fiber slant is somewhat random due to manufacturing tolerances. In the delivered array, the slant varies from 0 to +4 degrees, a large percentage being slanted about 2 degrees. The array as a whole was tilted 3 1/2 degrees with respect to the axis of the light source to obtain the effect shown in figure 17 for all but a few fibers. Experimental data indicates the dynamic range is about 32 db.

It is clear from the above discussion that fiber slant must be controlled within a few degrees to apply the technique of model 4, because it is necessary that the light source illuminate the same side of every fiber (upper side in figure 17) and because the array fibers cannot be tilted much more than 5 degrees otherwise light will pass through the array by reflection (ray C, figure 17). The delivered array is marginal in this respect, which led to the conclusion that model 4 could not be implemented. This was stated in Monthly Progress Report No. 3. Later observations made while the static masks were being prepared indicated that model 4 could be implemented over most of the array, with just a few fibers slanting too little.

If it is desired to center clip the signal spectrum, it can be accomplished by means of the geometry of figure 9 or 10 but with both masks displaced in opposite directions a small amount, S, so that no light is transmitted until the displacement equals S. The resulting transfer function is shown in figure 19. Symmetrical clipping occurs at a displacement equal to d-s. The equation of the transfer function is given below:

$$\frac{L}{I_o d\ell} = \frac{2}{\pi}\left(\frac{y}{d}\sin\theta - \frac{s\theta}{d}\right) \qquad (9)$$

where θ = arc cos s/y.

L = light flux transmitted

I_o = incident light intensity.

d = slit width in mask.

ℓ = length of fiber illuminated.

y = fiber peak displacement.

S = mask offset

Such a transfer function can be used to remove low level background noise. However, the dynamic range is poor.

The combined effects of diffraction and a finite source have only been estimated. The finite source tends to give the array a square law response. Diffraction also tends to give the array a square law response for small displacements. The combined response is probably approximately fourth power law for small amplitudes blending into square law for larger fiber amplitudes, than becoming linear as both source and diffraction effects become negligible.

Halation also tends to round off the response curve near the origin in a manner similar to mask offset. Halation is a photographic term describing the spreading effects that take place in photographic images due to diffusion of light in the emulsion during exposure. The masks are made by casting the shadow of the metal fiber array on photographic plate. As a result of halation, static mask slots tend to be slightly narrower than the shadow cast by the fiber. The effect is minimized by using Kodak High Resolution Plate for the static masks and by

controlling the exposure. Because of diffraction and finite source effects, the slot formed on the static mask can be either larger or smaller than the fiber width depending on the exposure. Also, the array can be tilted with respect to the light source so that the fibers cast a shadow wider than the fiber thickness. Therefore, halation can be compensated for.

The conclusions to be drawn from this discussion of the optical transfer characteristics of the array are that a small source should be used and model 4 should be implemented to obtain maximum dynamic range. For the dimensions used in the array delivered in Task I, 35 db dynamic range is theoretically obtainable. To implement model 4 successfully, the fiber slant must be controlled closely and in the future more effort should be made to control fiber slant.

35 db dynamic range is considered sufficient for many purposes, but could well be inadequate for use as a directly excited vibration sensor. For a further discussion of this, see section 2.3.3.

2.2.3 Sources of Noise With Steady State Signals

There are two noise phenomena that occur when complex steady state signals are applied to the array. These are called chopping noise and signal induced noise in this report. Chopping noise is discussed first. The light output of one

fiber varies with time essentially as sine squared if the fiber is treated as a square law detector. The average value of the light output represents the power spectrum. The ripple present has no significance (unless phase measurements are made), and should be filtered out. The method of doing this depends upon the method used to detect the array output. If the entire array output is detected simultaneously by photographic film, or some other photosensitive surface, the integrating properties of the photosensitive surface may be used to remove the ripple. The time constants must be longer than the fiber period for effective filtering. If the array output is scanned, the photodetector should dwell on each fiber at least for one fiber cycle. The detector output should be low pass filtered to remove the ripple component. The dwell time can be adjusted by varying the scan speed and the area of the array instantaneously viewed by the detector. Another alternative is very rapid scanning, a technique discussed at the end of this section.

Signal induced noise is a term used to describe fluctuations in a fiber's output as a result of two or more frequencies being impressed upon the fiber simultaneously. Suppose, for instance, two frequencies 2 Hz apart fall near the peak of a fiber Q curve, the fiber having a 20 Hz bandwidth. Since the frequencies are well within the fiber's bandwidth it is easy to see that the fibers amplitude will fluctuate just as

does the envelop of the input signal. Now, if one of the frequencies is far removed from the peak of the Q curve and the other is at the peak of the Q curve, the fiber amplitude will be more nearly constant but will still fluctuate. The maximum and minimum amplitude is just the sum and difference of the fiber amplitude when each signal is applied separately. If the input frequencies have equal amplitude and are 200 Hz apart, the maximum to minimum ratio is 1.1 in the above example. The delivered array is capable of resolving frequencies 60 Hz apart and has 20 Hz bandwidth fibers. The max. to min. ripple of a fiber to which it is applied one frequency at the peak of the Q curve and another 60 Hz away is 1.39. The ripple rate is 60 Hz. To remove this ripple, the photosensitive surface or photodetector should effectively low pass filter the array output at less than 60 Hz. Then frequencies separated 60 Hz or more will cause little signal induced noise and frequencies separated less will not be resolved.

If the array is scanned, the scanner should dwell on each fiber a time consistent with the bandwidths mentioned above. This imposes serious limitations on the scan speed. For example, say the 100 to 6000 Hz frequency range is scanned and the array has the characteristics given above. The scanner must dwell at least two ripple periods on each fiber for filtering to be effective. The reason is apparent from fig. 20, which shows the spectral components of a segment of the

fiber output two ripple periods long. A low pass filter with a cutoff of one-half the ripple period will pass the main lobe which is caused by the average value of the light pulse and exclude the main lobes caused by ripple, thus the filtering is fairly effective. A reduction in dwell time allows part of the main lobes caused by the ripple to be passed. Since a hanning window is much better than a rectangular window in terms of low side lobes and its smoothing properties, it should be used. Its physical width should be about three fiber spacings and its dwell time should be four ripple periods, for the same relationship of main lobes to hold as in figure 20. Thus, as shown in figure 20, the low pass filter should have a cutoff of one half the ripple frequency, or 30 Hz in the example being discussed. An equivalent alternative is to use a rectangular scan window three fiber spacings wide and a low pass filter whose frequency response is that of a hanning window. The rate of scan in fibers per second is found from the above relationships to be 3/4 the ripple frequency, or 45 fibers per second in the particular example. A 100 to 6000 Hz array with 20 Hz fiber spacings has 295 fibers, hence the time required to scan the array is 6.6 sec. This is intolerable for most applications.

A similar calculation may be made for the maximum scanning rate when only chopping noise is considered. In this case it is concluded that the maximum scan rate in fibers per second

equals 3/2 the fiber resonant frequency, and that the ideal low pass filter should have a cutoff equal to the fiber frequency. If a linear scan is used, the lowest frequency fiber determines the scan rate. To obtain a high scan rate hetrodyning may be used. The signal is frequency shifted so that the lowest frequency is rather high. The frequency shifted signal is analyzed by the array. For example, say the 100 to 4000 Hz band is to be analyzed. If the signal is analyzed directly, the scan rate is limited to 150 fibers per second. If the signal is shifted to the 2100 to 6000 Hz band, the maximum scan rate becomes 3150 fibers per second, a very significant improvement.

It is shown later that four arrays are necessary to cover the 100-20,000 Hz band. Using the design parameters of these arrays (see Section 2.4, Table of Design Parameters), and the scanning formulas derived above, the following scan time conditions are obtained:

Array	Minimum Scan Time To Remove Signal Induced Noise	Minimum Scan Time To Remove Chopping Noise
100-376 Hz	1.25 sec.	.185 seconds
276-1410 Hz	4.57 sec.	.185 seconds
1410-5320 Hz	4.34 sec.	.092 seconds
5320-20,000 Hz	4.07 sec.	.0457 seconds

In all cases, the minimum scan time to remove signal induced noise is too large unless it is known that the signals are essentially steady state or stationary.

A possible solution is to scan rapidly and average successive scans. Two techniques will be considered. In the first technique, the chopping noise is removed as before by a suitable choice of the scanner dwell time. To average out the signal induced noise, more than two scans per signal induced ripple period are necessary to satisfy the sampling theorem. If the ripple amplitude is just negligible at 200 Hz (it is ±5% for the lowest three arrays), then at least 400 scans per second are necessary (scan period $<$ .0025 sec.), so the maximum period set by signal induced noise and the minimum set by chopping noise are incompatible, thus the first technique will not work. It can be made to work over a limited frequency range by hetrodyning the signals up in frequency, but this is ruled out in the present application.

The second technique requires scanning at a rate more than twice the highest chopping frequency (to satisfy the sampling theorem). Even this may not be enough, because the fiber really full-wave rectifies the signal present on each fiber, hence the fiber output is described by a set of harmonics which fall off as $A_0 = 1$, $A_1 = 2/3$, $A_2 = 2/15$, $A_3 = 2/35$ etc. The scans must be averaged over at least one signal induced noise ripple period to remove signal induced noise. This technique requires very high scan rates and may be impractical, but is theoretically sound.

2.2.4 Higher Mode Response of Fibers

The first few resonant modes of a cantilever beam are shown in figure 21.[5] It is seen that the second and third mode frequencies are 6.27 and 17.55 times the fundamental. When the array is driven mechanically at the base, all of the modes are excited. One method of obtaining an unambiguous output is to band limit the signal being applied to the array so as to eliminate higher mode excitation. Another method of reducing the effects of a selected mode is to illuminate the fiber at a nodal point of the selected mode. Thus the effect of the second mode can be reduced by illuminating the fibers a distance .774 of the fiber length from the fixed end. If this technique is used, it is theoretically possible to cover an input frequency range at 17.55 to 1 in one array without ambiguity.

Fiber defects will in some cases shift the nodal point slightly, causing small ambiguities. The primary defect in fiber uniformity is caused by the process used to tune the arrays. It has been calculated that the response to the second mode cannot be reduced by more than a factor of 10 for this reason unless the nodal point of each fiber is measured and a masking technique used to illuminate each fiber at its nodal point. Even then there will be some response to second mode because of the finite width of the beam used to illuminate the nodal points. For these reasons the nodal point technique is

---

5. L.E. Kinsler and A.R. Frey "Fundamentals of Acoustics," John Wiley and Sons, N.Y. 1950, pp 83-87.

not recommended except possibly for very low frequency fibers which are large and can be accurately manufactured. Therefore for unambiguous outputs, it is necessary in general to limit the frequency band to a 6 to 1 range. The 100 to 20,000 Hz range be covered with at least three separate arrays covering roughly the ranges of 100 to 600 Hz, 600 to 3600 Hz and 3600 to 20,000 Hz. The signals being applied to these arrays must be band limited at the upper frequency of each range respectively to prevent second mode response.

Since the arrays are to be excited directly by some structural member, the band limiting must be accomplished by means of mechanical filters, the design of which is outside the scope of this report. It is probably necessary to cover the 100 to 20,000 Hz range with four arrays rather than three because of the filter design problems. In this case, each array would cover a 3.75 to 1 range, and the filters would attain about 40 db attenuation at 6 times the lowest frequency in the array.

2.3 Practical Design Factors Affecting Performance

2.3.1 Fiber Stress, Frequency Range, Dynamic Range

The fiber stress is a function of the resonant frequency of the fiber and the dynamic range that is to be obtained from it. This can be shown by deriving an equation for stress in terms of resonant frequency and fiber displacement. The derived equation will be presented without proof:

$$\sigma_{max} = 7.58\sqrt{E\rho}\, f_o\, y_o \qquad (10)$$

where σ_{max} is the maximum tensile stress in the fiber.

E is the modulus of elasticity, psi.

ρ is the density, $\frac{1}{388}\ \frac{lbs}{in^3}$

f_o is the fiber resonant frequency.

y_o is the fiber tip peak displacement.

Rectangular cross section assumed.

Thus, it is seen that the stress does not depend separately on the fiber width, thickness or length, but just on the resonant frequency, which in turn is a function of dimensions. For a given displacement, y_o, the fiber stress is proportional to frequency. The maximum displacement that can be obtained at a given frequency is set by the endurance limit of the fiber material. Arrays built to date have employed NI-SPAN-C, a spring material having an endurance limit of about 50,000 psi in the cold rolled, aged condition, a modulus of about 25 x 10^6 psi and a density of .293 lb/in^3. The fibers are .002 in. thick, the maximum useful displacement is .004 in. (model 4). This causes a stress of 28,000 psi in a 6000 Hz fibers. Adjacent fibers collide for a displacement of .004 in, but for very high input drive levels, the fiber displacement can reach .008 in. The fibers are separated .010 in, and the fibers have not been observed to vibrate beyond .008 in. The fiber stress is 56,000 psi for this displacement at 6000 Hz. Although this

exceeds the quoted endurance limit, no failures have been observed. Also it should be noted that the fibers are not aged, so the quoted endurance limit may be somewhat less than 50,000 psi.

The theoretical dynamic range of the 6000 Hz fiber is about 35 db as shown in Section 2.2.2. This is considered the maximum obtainable at 6000 Hz. The upper bound of the operating range is set by fiber stress, as shown above, and the lower bound is set by diffraction. The dynamic range obtainable at other frequencies is inversely proportional to frequency, assuming the lower bound remains fixed (as is reasonable). Therefore, the maximum dynamic range obtainable from the four arrays covering the frequency ranges 100-376 Hz, 376-1410 Hz, 1410-5320 Hz, and 5320-20,000 Hz is 59 db, 47 db, 37 db and 23 db respectively.

This statement is not exactly true because it is based on scaling of the present array design, in which hard limiting does not occur until the displacement is double the useful displacement. It might be possible to increase the dynamic range by 6 db if the fibers were spaced somewhat further apart and the fiber limiter shown in figure 22 were used. The idea is to make the stress at the maximum useful displacement equal the endurance limit (50,000 psi), but not permit larger displacements. This idea probably would have to be used on the high frequency array simply to keep the fiber spacings large enough to implement the tuning procedure now in use.

2.3.2 Factors Affecting Fiber Bandwidth

Fiber bandwidth arises from three causes. These are aerodynamic damping, fiber hysteresis damping and hysteresis damping in the base material in which the fibers are embedded. An exact analysis of these sources of damping would be very difficult. However, an approximate analysis is possible and combined with experimental data, allows design formala to be obtained.

Aerodynamic damping will be considered first. As can be seen from figures 1 and 2 the fiber has a paddle like shape. When it vibrates, aerodynamic drag damps the fiber. This effect is enhanced by placing the static mask close to the fibers, because this increases the air velocity around the fibers. An approximate expression for bandwidth in terms of fiber geometry has been obtained. It shows that the bandwidth is independent of frequency. First the fiber Q is expressed as

$$Q = \frac{\omega_o U}{P} \qquad (11)$$

where ω_o is the radian resonant frequency.

U is the stored energy of the fiber.

P is the power loss (due to damping).

Each element of length of the fiber contributes an increment of stored energy given by $dU = \frac{1}{2} \rho A v^2 dx$

where ρ is the fiber density

A is the fiber cross section.

v is the peak velocity of the fiber at a distance x from the base.

dx is the increment of length.

Because the fiber velocity is very low, the drag force is proportional to the fiber velocity (this is the Stokes region of flow). Therefore the power loss due to element dx is given by

$$dP = \frac{1}{2} k v^2 dx$$

where k is a constant dependent on geometry and the viscosity of air, and where the flow is assumed to be in a plane perpendicular to the fiber.

The ratio of dU to dP is

$$\frac{dU}{dP} = \frac{\rho A}{k} = \frac{U}{P}$$

where the last equality follows because $\frac{dU}{dP}$ is a constant. Therefore Q is given by

$$Q = \frac{\omega_0 \rho A}{k} \tag{12}$$

and the bandwidth B is given by

$$B = \frac{f_0}{Q} = \frac{k}{2\pi\rho A} \tag{13}$$

Thus bandwidth is independent of frequency. This derivation neglects end effects. It has been experimentally verified over a 200 Hz to 6000 Hz frequency range using an array of the type delivered on this program. It has been verified for round fibers over a 200 to 10,000 Hz frequency band. Experiments show that the bandwidth varies inversely with mask to fiber clearance, the clearance being .0015 inches for 20 Hz.

The effect of hysteresis losses in the fiber material may be derived accurately. The Q is written as

$$Q = \frac{\omega_0 U}{P} = \frac{2\pi U}{\Delta U} \tag{14}$$

where ΔU is the energy lost per cycle due to hysteresis. Considering an arbitrary element of volume of the fiber, the energy density is proportional to the strain squared. Likewise, the energy loss per cycle per unit volume is proportional to the strain squared. Hence,

$$\frac{\frac{dU}{dV}}{\frac{d\Delta U}{dV}} = \text{constant} = \frac{U}{\Delta U} = \frac{Q}{2\pi} \tag{15}$$

where dV is an element of volume. Therefore the fiber Q due to hysteresis alone is a constant dependent on the material. The Q of NI-SPAN-C is quoted to be as high as 8000. If a figure of 5000 is used, the bandwidth at 20,000 Hz due to fiber hysteresis would be 4 Hz. This is small compared to the design goal which is 20 Hz or more. At lower frequencies, the contribution to bandwidth of fiber hysteresis is even less, and therefore can be ignored over the entire frequency range.

Base material hysteresis losses may be analyzed in a similar manner. Again the fiber Q is expressed as in equation 14. The stored energy and loss per cycle in the base are calculated as a function of fiber length. For constant fiber displacement, it is clear that:

Base strain $\propto \frac{1}{\text{fiber length}}$

Total strain energy of fiber $\propto$ (fiber length) $(\text{strain})^2 = \frac{1}{\text{fiber length}}$

Base loss per cycle $\propto (\text{strain})^2 \propto \frac{1}{(\text{fiber length})^2}$

Q Base $\propto \frac{U}{\Delta U} \propto$ fiber length $\propto \frac{1}{\sqrt{f}}$

$$B = \frac{f}{Q} \propto f^{3/2} \qquad (16)$$

The proportionality constant depends on the base material and the distribution of stresses in the base material. It also depends in a critical manner on the bond strength between the fiber and the base according to data taken on experimental arrays.

Measurements were made, in an earlier program, in an attempt to evaluate the three sources of loss discussed. To evaluate base losses, NI-SPAN-C fibers were potted in epoxy, a relatively lossy material. The 3/2 power law (equation 16) was verified to be reasonably accurate (measured power = 1.4). Also an array similar to the type delivered in Task I was placed in a vacuum to eliminate air damping. Bandwidth was found to increase linearly with frequency, 6 Hz being measured at 6000 Hz. Because the quantity of data taken was small (20 measurements on one array), the 3/2 power will be used to extrapolate the hysteresis losses to 20,000 Hz. The extrapolated bandwidth (extrapolated from 6000 Hz) is 36 Hz. A linear extrapolation gives 20 Hz.

The bandwidth due to base losses may be reduced by reducing fiber thickness. A scaling law indicates that the bandwidth due to base hysteresis is proportional to the square root of fiber thickness. Therefore, a reduction from .002 to .001 inches would reduce the base bandwidth from 36 to 25 Hz.

The bandwidth due to base hysteresis varies more from fiber to fiber than does the bandwidth due to air damping. This is so because base damping depends critically on the fiber to base bond strength. Variations of ±30 percent are common. Whether these variations are acceptable depend upon the use put to the output data from the array. If the frequency range were reduced down to 10,000 Hz, hysteresis would contribute 12 Hz to the bandwidth and the variations in bandwidth due to hysteresis would be quite small compared to the 20 Hz bandwidth which would probably be used.

2.3.3 Vibration Levels Needed to Drive Array

If the signal is of the discrete frequency type, the vibration level needed to drive the array may be found simply from the transfer function given in figure 8. It was shown that the fiber tip displacement is Q times the base motion at resonance. Therefore, the base motion required is

$$y_{base} = \frac{y_{tip}}{Q} = \frac{B\, y_{tip}}{f} \qquad (17)$$

where B is the fiber bandwidth at frequency f. If the fiber bandwidth is independent of frequency as is the case for the array delivered in Task I, then, to maintain constant fiber tip motion, the base drive level must vary inversely with frequency.

The fiber tip motion due to a random signal may be found in terms of the power spectral density of the input signal. Since the input is in terms of base displacement, y_b, the input spectral density is given by

$$P_{base}(f) = \lim_{T\to\infty} \frac{1}{T} \left| \int_{-T}^{+T} y_b(t)\, e^{-j\omega t}\, dt \right|^2$$

and has units of $(\text{inch})^2$ sec = $(\text{inch})^2/\text{Hz}$. The rms fiber tip displacement is given by

$$(y_{tip\,rms})^2 \simeq P_{base}(f) \cdot \int_{-\infty}^{+\infty} |H(\omega)|^2\, df$$

where $H(\omega)$ is the fiber transfer function (figure 9). When this integration is carried out it is found that

$$(y_{tip\,rms})^2 = \frac{\pi}{2} Q^2 B\, P_{base}(f)$$

$$y_{tip\,rms} = \sqrt{\frac{\pi}{2}}\, \frac{f[P_{base}(f)]^{1/2}}{B^{1/2}} \qquad (18)$$

where B is the 3 db bandwidth at frequency f and P_{base} is the single sided power spectrum.

If the input is given in terms of acceleration measured in g's, then the input power spectral density will be in terms of g^2/Hz. The fiber tip motion is then given by

$$y_{tip\,rms} = \frac{388}{(2\pi f)^2}\left(\frac{\pi}{2}\right)^{1/2}\frac{f\,P^{1/2}}{B^{1/2}} = \frac{12.3\,P^{1/2}}{f\,B^{1/2}} \qquad (19)$$

where P is measured in g^2/Hz

An example application of this equation is now presented. Say the fiber bandwidth is 20 Hz, the frequency is 2000 Hz and the power spectral density is $1\ g^2$/Hz. The fiber tip motion is given by

$$y_{tip\,rms} = \frac{12.3 \cdot 1^{1/2}}{2000(20)^{1/2}} = .0014 \text{ inches.}$$

This motion is within the dynamic range of the fiber.

The small dynamic range of the arrays (23 to 41 db) makes it necessary to control the input vibration level accurately, otherwise the array output will be badly distorted or absent entirely. The large frequency range to be covered (100 Hz to 20,000 Hz) aggrevates this problem. In previous applications, it has been found necessary to record the signals on magnetic tape, and excite the array with an electromechanical driver. The signal is played several times in order to optimize the drive level. Slope networks are used to compensate for the characteristics of the driver and also the characteristics of the signal. The slope networks are often essential even when covering the 100 Hz to 4000 Hz frequency band. Automatic gain control circuits have sometimes been used to maintain the input

drive level within narrow limits. In another application, the total light output of the array was maintained at a predetermined level by means of a photocell which was connected to a fast acting automatic gain control circuit which was part of the signal amplifier chain. Without such procedures the performance of the array is likely to be poor. It is difficult to see how such procedures or equivalent procedures can be implemented when the input signal is in the form of a structural vibration which is applied directly to the array.

2.3.4 Static Displacement of Fibers in Array Undergoing Acceleration

In the intended application, it is understood that the array will be subjected to steady state accelerations as high as 5 g. If the array is mounted so that the direction of vibration and direction of steady state acceleration coincide, the fibers will be displaced relative to the static mask. This effect may be analyzed in terms of the transfer function (figure 8) which is accurate at zero frequency. The analysis is given below. The fiber transfer function is

$$H(\omega) = \frac{-jQ\,\omega/\omega_0}{1+jQ\left(\omega/\omega_0 - \frac{\omega_0}{\omega}\right)} \qquad (20)$$

$$H(\omega_0) = -jQ$$

$$H(0) = \lim_{\omega \to 0} \left(\frac{\omega}{\omega_0}\right)^2$$

$$y_{tip}(\omega_0) = -jQ\,\frac{\ddot{y}_{base}(\omega_0)}{\omega_0^2} \qquad (21)$$

$$y_{tip}(0) = \lim_{\omega \to 0} \left(\frac{\omega}{\omega_0}\right)^2 \frac{\ddot{y}_{base}(\omega)}{\omega^2} = \frac{\ddot{y}_{base}(0)}{\omega_0^2} \qquad (22)$$

$$\frac{y_{tip}(\omega_0)}{y_{tip}(0)} \simeq -jQ \frac{\ddot{y}_{base}(\omega_0)}{\ddot{y}_{base}(0)} \qquad (23)$$

If the AC signal is random at ω_0, then $\ddot{y}_{base}(\omega_0)$ is given by

$$\ddot{y}_{base}(\omega_0) = \left[\frac{\pi}{2} B P_{base}(f_0)\right]^{1/2} \qquad (24)$$

where B is the fiber 3 db bandwidth.

P_{base} is the single sided power spectrum in units of (acceleration)^2/Hz.

$y_{tip}(\omega_0)$ is the rms displacement.

An example calculation is given

$P_{base}(f_0) = 1\ g^2/Hz$

$B = 20Hz$

$\ddot{y}_{base}(0) = 5g$

$f_0 = 100Hz$

$\ddot{y}_{base}(\omega_0) = \left(\frac{\pi}{2} B P_{base}\right)^{1/2} = 5.61\ g^2/Hz$

$Q = f_0/B = 5$

$y_{tip}(\omega_0)/y_{tip}(0) = -j5\ \frac{5.61}{5} = -j5.61$

$y_{tip}(0) = \ddot{y}_{base}(0)/\omega_0^2 = \frac{5 \times 388}{(2\pi \times 100)^2} = .005$ inches

In view of the fact that the fiber thickness in the standard array is .002 inches, the static displacement is much too large. The frequency at which the static displacement is negligible (70 microinches) is, from equation 22, 850 Hz.

A possible solution to this problem is to mount the array at right angles to the acceleration vector. This is unacceptible if it is the vibration components parallel to the acceleration vector which are of interest.

A possible method of mounting the array which isolates it from the steady state acceleration, yet applies the vibration component parallel to the acceleration vector to the array is shown in figure 23. The array fibers are parallel to the acceleration, hence are not displaced statically. The resonant frequency of the array mounted on leaf springs is placed well below the lowest frequency of interest. A vibration parallel to the acceleration vibrates the array along the X axis because the mass of the array tends to remain stationary. A vibration in the X direction also has an effect on the array, the decoupling depending on the design of the springs. Whether these are satisfactory solutions cannot be answered without more information on the intended use of the array.

2.3.5 Magnetic Coupling Between Fibers

If the fibers are made of a magnetic material, magnetostatic forces can exist between them. These forces can have a

very large effect if a highly magnetic material such as carbon steel is used for the fibers. The arrays built to date use NI-SPAN-C, a material having a relatively low saturation induction of 500 gauss.

A useful model in analyzing one type of magnetic coupling effect is shown in figure 24. The fiber mass is represented by m, the fiber spring constant by spring k and the magnetic coupling by spring k_c. The physical situation giving rise to this model is also shown in Figure 24. The applied magnetic field, B_o, causes magnetic poles to be induced in the fiber tips. These poles repel each other. If a fiber is displaced from its rest position, these magnetic fources cause a restoring force on the fiber, and also a coupling force on the adjacent fibers. These forces can be represented by a spring as in figure 24. If the applied magnetic field is sufficient to saturate the fibers then an approximate expression for the spring constant associated with magnetic coupling can be derived easily. It is

$$K_C = \frac{B_s^2 ab}{2\pi\mu_o s^2} \qquad (25)$$

where the dimensions are shown in figure 24.

B_s is the saturation induction.

μ_o is the permeability of free space

MKS units are used.

Likewise, the fiber mass and spring constants, are given, as stated in figure 8, by

$$K = \frac{3EI}{\ell^3}$$

$$m = .226 \rho A \ell$$

The ratio of $\frac{k_c}{k}$ can be reduced to

$$\frac{k_c}{k} = .63 \frac{\beta_s^2 b^{1/2}}{\mu_o E^{1/4} \rho^{3/4} s^2 \omega_o^{3/2}} \qquad (26)$$

where E is the modulus of elasticity.

ρ is the density.

ω_o is the resonant radian frequency.

MKS units are used

In general, each section of the mechanical filter is different since each fiber is tuned to a different frequency. If each fiber were identical, then the passband characteristics of the filter can be easily derived from image parameter theory. It is useful to calculate the bandwidth of the filter under this assumption because it gives a good measure of the coupling effects. Assuming in addition that the fiber damping is negligible, it can be shown that

$$f_\pi - f_o = f_o\left(\sqrt{1 + 4\frac{k_c}{k}} - 1\right) \qquad (27)$$

where f_π is the upper cutoff.

f_o is the lower cutoff, and is also the fiber resonant frequency in the absence of coupling.

The subscripts, π, 0, signify the phase shift per section.

An example calculation is given, using the dimensions of the array delivered in Task I.

Material: NI-SPAN-C.

Fiber Thickness, b = .002 inches

Fiber Width, a = .022 inches

Fiber Frequency, = 2000 Hz

$$\frac{k_c}{k} = .035$$

$$f_\pi - f_o = 2000\left(\sqrt{1+4\times.035}-1\right) = 142\,Hz$$

Since the bandwidth of the filter is large compared to the fiber spacing of 20 Hz, it is concluded that the coupling affects will have a pronounced effect on the fiber's transfer characteristics. This has been observed experimentally. The resulting fiber transfer characteristics when the arrray is driven in the usual manner at the base has been observed to have a bandwidth roughly equal to the predicted value of 142 Hz, but it has several pronounced peaks and valleys. The peaks and valleys are the result of driving each section of the filter rather than just one input section. A particular fiber's output is the superposition of several waves arriving at the fiber at various phases dependent on frequency. Of course, it is necessary to apply a magnetic field to the array to observe these effects. Under normal conditions, no coupling is observed.

In addition to coupling, a magnetic field applied parallel to the fibers raises the resonant frequency of the fibers. This effect is negligible for the small fields normally present around the array (say under 10 gauss).

When the applied field is transverse to the array as shown in figure 25, the fibers tend to stick to each other. Experience has shown that this effect is very troublesome with thin fibers (.0005 thick) at low frequencies. Furthermore, with such fibers, the residual magnetism is sufficient to keep the fibers clumped after the applied field is removed. A theoretical analysis of this effect is too difficult to carry out completely, however, some useful information may be derived. Consider the effect of changing just the fiber length. Assume the fibers become saturated when they touch (a worst case condition). Then magnetic force is independent of ℓ and f. The spring constant is proportional to one over length cubed. This is illustrated grapically in figure 25. It is seen that for frequencies below some critical frequency, clumping will occur (given an applied field sufficient to saturate the fibers). This critical frequency can be calculated roughly, assuming sufficient field is applied to cause saturation. The derivation will only be outlined: The magnetic force holding the fibers together is approximately

$$F_m = \frac{1}{2} \frac{ab B_s^2}{\mu_0} \qquad (28)$$

where ab is the fiber cross section. This formula is based on the fact that the flux in the fiber is largely axial due to the high depolarization factor in the axial direction. The force cannot be greater than the above value since this is the force that would be exerted in the fiber tip if all the flux excited there. The spring restoring force is, from figure 8.

$$F = \frac{KS}{2} = \frac{3}{2}\,\frac{EIs}{\ell^3} \tag{29}$$

These forces are equated, and solved for ℓ. Then ℓ is replaced in the equation for resonant frequency (figure 8). The frequency below which clumping occurs is found to be

$$f_{clamp} = \frac{.4\,B_s^{4/3}}{\mu_o^{2/3} E^{1/6} \rho^{1/2} b^{1/3} S^{2/3}} \tag{30}$$

where B_s is the saturation induction.

μ_o is the permeability of free space.

E is the modulus of elasticity.

ρ is the density.

b is the fiber thickness.

S is the fiber spacing.

Mks units are used.

For NI-SPAN-C fibers, the equation can be reduced to

$$f_{clamp} = \frac{400}{b^{1/3} S^{2/3}} \tag{31}$$

where b and s are measured in thousandths of an inch. If the fiber thickness is 2 thousandths and the fiber spacing is 10 thousandths, as in the delivered array, the calculated clumping frequency is 70 Hz. Therefore it is concluded that clumping is not a problem covering the 100 Hz to 20,000 Hz band, even with the fiber cross section presently used in arrays.

2.3.6 Critical Dimensions. Thermal Expansion Problems. Tuning Accuracy.

The critical dimensions of the array assembly delivered in Task I will be discussed because the problems encountered are typical. The active part of the array is 2.0 inches long. It contains 200 fibers each with a cross section of .0020 x .022 inches. The array covers a frequency range of 2000 to 6000 Hz. The fiber length varies from .098 to .170 inches. The static mask to fiber clearance is .0015 inches, which results in a fiber 3 db bandwidth of 20 Hz. It is estimated that the clear slots in the static mask are lined up with the fibers within 35 microinches. The fibers are tuned to an accuracy of ±2 Hz. After the array has been used, the accuracy at the low end of the array remains unchanged, but at the high end a small percentage of the fibers drift. The accuracy at the high end is about ±5 Hz for these few fibers and remain ±2 Hz for the majority.

The criticalness of each of these dimensions will be reviewed briefly.

2.3.6.1 Number of fibers per inch (100 in example).

The fiber spacing is held to .010 ±.0002 at the base because it is easy to do. However errors of ±.001 would not seriously affect performance. Errors in spacing would affect the frequency linearity of the array if the frequency spacing between adjacent fibers were held constant. Errors in spacing

produce errors in the smoothed (over frequency) amplitude output of the array (see Section 2.2.1). These errors are considered to be negligible in the delivered array.

2.3.6.2 Fiber Thickness.

The fiber thickness is critical because it affects the frequency of the fibers before tuning (see figure 8). An attempt is made to hold the fiber thickness to .002 ±10 microinches. A 10 microinch error causes a 1/2 percent frequency error before tuning (30 Hz at 6000 Hz).

2.3.6.3 Fiber Width

The array width is held to .0220 ±0005. The width is not critical, however, the flatness on the sides is because of the small clearance between the array and static masks.

2.3.6.4 Fiber Length.

The fiber length is critical because of its effect on frequency before tuning. By differentiating the frequency equation of figure 8, it is found that

$$\frac{\Delta f}{f} = -2\,\frac{\Delta \ell}{\ell}$$

The frequency errors are seldom more than 100 Hz at 6000 Hz before tuning. If the entire error is due to length, then the length is being held to about .001 inches.

2.3.6.5 Mask to Fiber Clearance.

The mask to fiber clearance largely determines fiber bandwidth. Bandwidth varies inversely with clearance, so the clearance is critical. The clearance of .0015 on each side adds up to .003 inches. It is the sum of clearances that is really critical. This is important because the array tends to develop a slight chamber after it is removed from the surface grinder use to render the sides flat. The clearance is held accurately at the array ends by means of .0015 thick shims. A slight chamber in the array can be tolerated. The static masks, however must be flat. Care must be used not to bend them while they are being bonded in place.

2.3.6.6 Alignment of Static Mask Slots with Fibers

The alignment is performed under a microscope by means of an optical alignment fixture. The fixture consists of a small light source and collimating lens. The array is illuminated with collimated light, which makes a small angle with respect to the fibers (see figure 17). First one mask is placed in the array assembly and aligned (as viewed by the microscope). The effects of diffraction discussed in section 2.2.2 are readily observable. The microscope is focused on the emulsion of the static mask. The fiber being viewed slants, therefore only one edge of the fiber will be illuminated. The mask is aligned with this edge. The mask is bonded to the metal housing with epoxy. It is room cured to avoid thermal expansion

problems. Alignment after curing has been found to be very good. The procedure is repeated with the other mask.

2.3.6.7 Differential Expansion.

Differential thermal expansion limits the temperature range which the array assembly can be subjected to. Static mask alignment is the limiting factor. From the discussion of diffraction effects, it was concluded that the dynamic range is 35 db, and the smallest perceptible fiber motion is about 70 microinches for the delivered array. Since gross mask misalignment degrades dynamic range even further, a mask misalignment of 35 microinches due to thermal expansion will be used as a design criterion. The material used in the construction of the delivered array and their expansion coefficients are:

Part	Material	Expansion Coefficient, deg F^{-1}
Fiber	NI-SPAN-C	4.5×10^{-6}
Array Base	Pure nickel	7.2×10^{-6}
Housing	Precipitation hardening stainless steel	5.6×10^{-6}
Static Mask	High Resolution Kodak Plate	4.5×10^{-6}

The array is bonded to the housing with epoxy and the masks are bonded to the housing with epoxy. It is initially assumed that the array and masks are bonded just at the centers, so the length used in the calculations is 1 inch (1/2 the array length). The differential expansion between

array and static mask will be 35 microinches for a temperature change of 13 degrees F, a relatively small change in temperature.

To extend the temperature range somewhat, the array is in fact bonded over its entire length to the housing. The housing is much more massive than the array, so the array is constrained to expand with the housing provided the epoxy used is stiff enough to transmit the shear load. If this assumption is made, and the masks are bonded just at the center, then the temperature change becomes 32 degrees F for a differential expansion of 35 microinches. The temperature range would then be 38 to 102 degrees F. This is enough for some applications.

To extend the temperature range further, the static masks might be bonded to the housing over their full length. The epoxy must be cured at room temperature, otherwise differential expansion that occurs during curing will be locked in. On the other hand, good high temperature properties are not obtained with a room temperature cure. These difficulties are not insurmountable, but require further work. A possible solution is to use a housing material which matches the masks more closely, NI-SPAN-C, for instance. The array could be electron beam welded to the housing, thus obtaining a stable high temperature bond. The masks would be epoxy bonded to the housing either at their centers or over their full length. Now, however, a high temperature cure is possible because of the good thermal expansion match between the masks and housing. The

maximum temperature will be determined by the softening temperature of the epoxy, or possibly by the small remaining difference in expansion coefficients. The maximum temperature could be on the order of 170 degrees F. The minimum temperature would probably be set by differential expansion. It might be about -30 degrees F. This assumes the present differential expansion is reduced by a factor of three.

The 100 to 20,000 Hz arrays will now be considered. It will be assumed that the minimum perceptible fiber motion is the same for all arrays (70 microinches), and that the allowable differential expansion is 35 microinches. From Section 2.4, the array lengths are .56, 2.06, 1.95, and 1.83 inches progressing from low to high frequency. Since the upper three arrays have approximately the same lengths, they will cover the same temperature ranges. The lowest array is shorter by a factor of 3.6. It will tolerate 3.6 times the temperature change, if differential expansion sets the limit. Assuming the upper three arrays cover a -30 to 170 degree F range, the lowest array would cover a -270 to 170 degree F range.

2.3.6.8 Fiber Tuning Accuracy.

The discussion of tuning accuracy will be concerned with an extrapolation of the present technique up to 20,000 Hz, since no serious difficulties exist at frequencies below 6000 Hz, based on previous experience. A 6000 Hz fiber has a length of .098 inches in the current array design. If the frequency range

is extended to 20,000 Hz simply by use of shorter fibers, then the fiber length at 20,000 Hz will be .054 inches. It has been concluded that the primary source of error before tuning is fiber length, and that fiber length can be held to ±.001 inches. This figure is not likely to be improved upon. Although the frequency error before tuning will be about 180 Hz at 20,000 Hz, the length error will be the same, and therefore the time required to abrade away excess material on the fiber will not change.

The primary problem if any in tuning the 20,000 Hz fibers will be in achieving high accuracy. The amount of material corresponding to a 2 Hz change at 20,000 Hz is less than that at 6000 Hz by a factor of 1.83. Therefore it is expected that the accuracy at 20,000 Hz will be about 2 x 1.83 = 3.7 Hz on the average. A few fibers will be in error by about 9 Hz rather than 5 Hz at 6000 Hz. These errors are considered acceptible.

Thinner fibers might be used in the high frequency array. This does not materially affect the conclusions reached above.

2.3.7 Structural Resonances

The array assembly delivered in Task I consists essentially of an array, static masks and a housing. The assembly has many modes of vibration, which are determined primarily by the housing. The lowest mode is the flexural mode. Calculations indicate this mode will be at about 10 Kc. This is sufficiently above the highest fiber frequency to be of no consequence.

Of the arrays necessary to cover the 100 to 20,000 Hz frequency range, only the highest will present a new structural resonance problem. It presents a severe problem because it is not only larger, but also the array frequencies are higher.

A failure to place the structural resonances above the highest frequency of the array would in many instances cause the array response to be very nonuniform versus frequency in the vicinity of resonance. This is not the case for all resonances, however it is considered good practice to place the resonances above the array frequency range if possible.

First the longitudinal resonances will be considered. Within the band longitudinal resonances are not acceptable in the array assembly because they couple well to the fibers. If the housing is made of steel, steel alloy, nickel, or aluminum, the longitudinal velocity of sound in the housing will be about 2×10^5 inches/seconds. The wavelength at 20,000 Hz is 10 inches (velocity divided by frequency). When the housing is not bolted down, that is when it is suspended freely, it will resonate in the longitudinal mode at 20,000 Hz if it is 5 inches long (1/2 wavelength). Any increase in length will reduce the resonant frequency. The longitudinal mode has a node at the middle of the housing and maxima at each end. Hence, if the housing is bolted down at the ends to a large structure, it will not be able to resonate on its own in this

mode. However, the large structure must have resonances of its own which are even lower in frequency. If the housing is bonded along its entire length to a large structural member then it will be constrained to vibrate with the structural member. At high frequencies, longitudinal standing waves are likely to exist in the structure. If the array is an appreciable fraction of a wavelength, the input displacement of the fiber will vary over the array length, probably by a large amount.

It is not possible to fully evaluate the resonances in a structural member by making measurements just at one point; it is necessary to make sufficient measurements to locate all the nodes and maxima. To do this, it is desirable that each vibration sensor measure the vibration over a small area of the structure rather than over a large area of the structure. The latter requirements can be approximated by the metal fiber array if it is attached to the structure undergoing test at one end of the array or in the middle, and if the structure is massive enough to be almost unperturbed by the array. In this case, the resonances of the array assembly can be considered independently of the resonances of the structure undergoing test. If the array is attached at one end, it will resonate at a frequency such that it is 1/4 wavelength long. Therefore the 5320 to 20,000 Hz array must be less than 2 1/2 inches long. However, if it is attached at its middle, then it will

resonate when it is 1/2 wavelength long, 5 inches at 20,000 Hz. Since the mechanical Q of this resonance will be very high, it is sufficient to place the resonance just above 20,000 Hz.

Flexural resonances couple weakly or not at all to the fibers. As a matter of conservative design practice, the flexural resonances should be placed above the frequency band covered by an array if possible. It is possible in all but the highest frequency array. This array will undoubtedly have two or more transverse resonances.

The 5 inch limitation on array length for the 5320 to 20,000 Hz array has a considerable effect on array design. For instance, if the fiber spacing is 20 Hz and there are 100 fibers per inch (as in the 2000 to 6000 Hz array), the length would be 7.3 inches. Due to the method of manufacture, the physical spacing between fibers cannot be reduced unless the fiber thickness is reduced. If the fiber thickness is reduced to .001 inches, from .002 inches, the array length would be 3.7 inches, an acceptable length.

2.4 Rough Design of Arrays to Cover the 100 Hz to 20,000 Hz Frequency Range

This section presents the rough designs of the arrays necessary to cover the 100 Hz to 20,000 Hz frequency range. It is summary in form since the basic information is also contained in Section 2.2 and 2.3.

Four arrays are necessary to prevent higher mode excitation (Section 2.2.4). They would cover frequency ranges of 100 to 376 Hz, 376 to 1410 Hz, 1410 to 5350 Hz and 5320 to 20,000 Hz. All the arrays would use the construction techniques which were used to manufacture the array delivered in Task I, which covered the 2000 to 6000 Hz range. The lowest four arrays could use .002 inch thick by .022 inch wide fibers. Probably the lowest array would use fibers several times as thick to improve dynamic range. Thicker fibers could also be used in the 376 to 1410 Hz array. Note, however, that the greater dynamic range obtained can only be taken advantage of if the signal spectrum is strong enough, since it is the upper bound of the range that is increased.

The highest array would use .001 inch thick fibers spaced .005 inches. The reason for this is to reduce somewhat the base hysteresis losses (see Section 2.3.2), and more importantly to reduce the array length so as to prevent longitudinal resonances from occurring below 20,000 Hz (see Section 2.3.7). A fiber limiter is necessary (Section 2.3.1).

The fiber frequency spacings and bandwidths would be about as follows: The three lowest arrays would have fiber bandwidths of about 20 Hz. This could be modified somewhat to suit the customer. The two lowest arrays would have fiber spacings of 1/2 bandwidth. The reason is that these arrays have few fibers in them anyway (28 and 103 for 1/2 bandwidth

spacing), and therefore the improved performance seems worth the extra fibers (see Section 2.2.1 on resolution and spatial smoothing of optical output). The 1410 to 5320 Hz array would have fibers spaced one bandwidth because a closer spacing would cost more than its worth (in our opinion). The high frequency array would have fibers spaced 20 Hz or more apart. Because the high frequency array covers 3.76 times the frequency range covered by the other arrays combined, it will contain 3.76 times as many fibers if the same fiber spacing is used. Therefore its cost will be much greater than the other arrays. This problem can be alleviated somewhat by using more fiber bandwidth and spacing the fibers farther apart in frequency. A fiber bandwidth and spacing of 40 Hz is recommended. Whether this is acceptable depends on the signal spectrum being analyzed. Specifically, it depends on the resolution required and upon the magnitude of the spectral density. If the larger bandwidth is used the length of the array would be reduced from 3.7 inches to 1.85 inches and the number of fibers would be 370.

The dynamic range of the arrays would be about 41 db for the two lowest arrays (assuming .004 inch thick fibers are used) and 35 db for the 1410 to 5320 Hz array. It would be 23 db for the high frequency array.

The temperature range over which the arrays would operate are estimated to be about -270 to 170 degrees F for the lowest array and -30 to 170 degrees for the other arrays, based on

differential expansion. Other phenomena might set a limit higher than -270°F.

The tuning accuracy would be ±2 Hz on the average for the lowest three arrays and ±5 Hz on the average for the high frequency array.

The lengths of the arrays would be about .5, 2, 2, 2 inches respectively from low to high frequency assuming fiber thickness of .004, .004, .002, .001 inch respectively and bandwidths of 20, 20, 20, 40 Hz respectively.

This information and some additional information is summarized in the following table:

TABLE OF DESIGN PARAMETERS

	ARRAY			
	100 to 376	376 to 1410	1410 to 5320	5320 to 20,000
Fiber bandwidth, Hz	20	20	20	40
Fiber spacing, Hz	10	10	20	40
Fiber thickness inches	.004	.004	.002	.001
Fiber spacing, inches	.020	.020	.010	.005
Frequency range, Hz	276	1034	3910	14,680
Number of fibers	28	103	195	366
Active length, inches	.56	2.06	1.95	1.83

TABLE OF DESIGN PARAMETERS (Cont'd)

	ARRAY			
	100 to 376	376 to 1410	1410 to 5320	5320 to 20,000
Temperature range, degree F	-270[6] to 170	-30 to 170	-30 to 170	-30 to 170
Frequency resolution	30	30	60	120
Aliasing error	< 2%	<2%	<14%	<14%
Dynamic range, db	41	41	35	23
Minimum observable fiber motion, inches	70×10^{-6}	70×10^{-6}	70×10^{-6}	70×10^{-6}
Maximum usable fiber motion, inches	.008	.008	.004	.0012
Input range, micro-inches				
100 Hz	14-1570			
376 Hz	3.76-460	3.76-460		
1410 Hz		1-112	1-56	
5320 Hz			.266-15	.532-7.5
20,000 Hz				.14-2

The frequency resolution given in the table is based upon the discussion of smoothing in Section 2.2.1, and the aliasing error is also. The aliasing error refers to the difference between the peak values of the spatially smoothed array output when the input frequency falls at a fiber frequency and when it falls midway between two fibers.

The input range refers to the peak input displacement defining the lower and upper bounds of the dynamic range of the array.

6. Based on differential expansion. Other phenomena will probably set a higher limit.

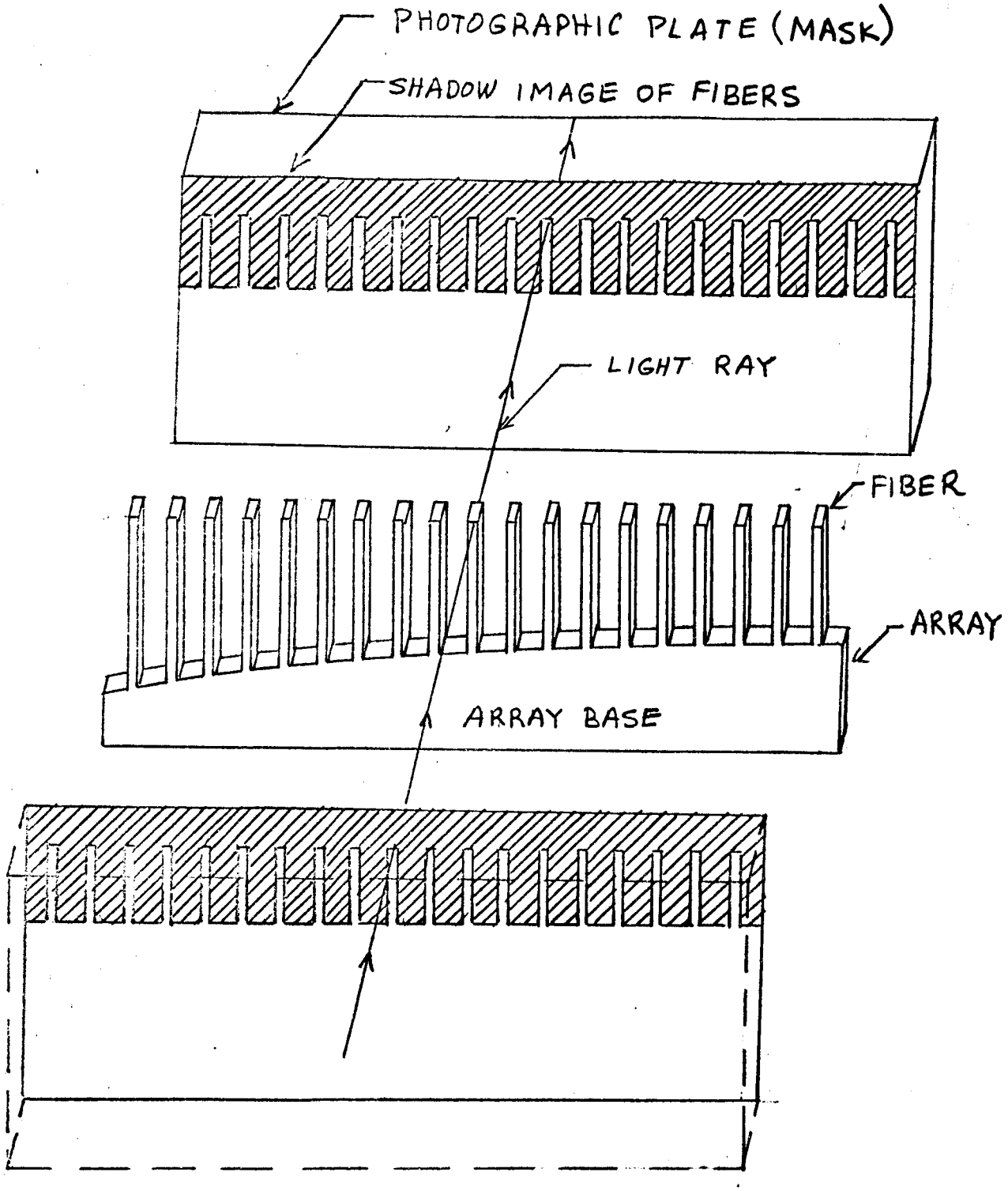

FIGURE 1- ARRAY AND MASKS

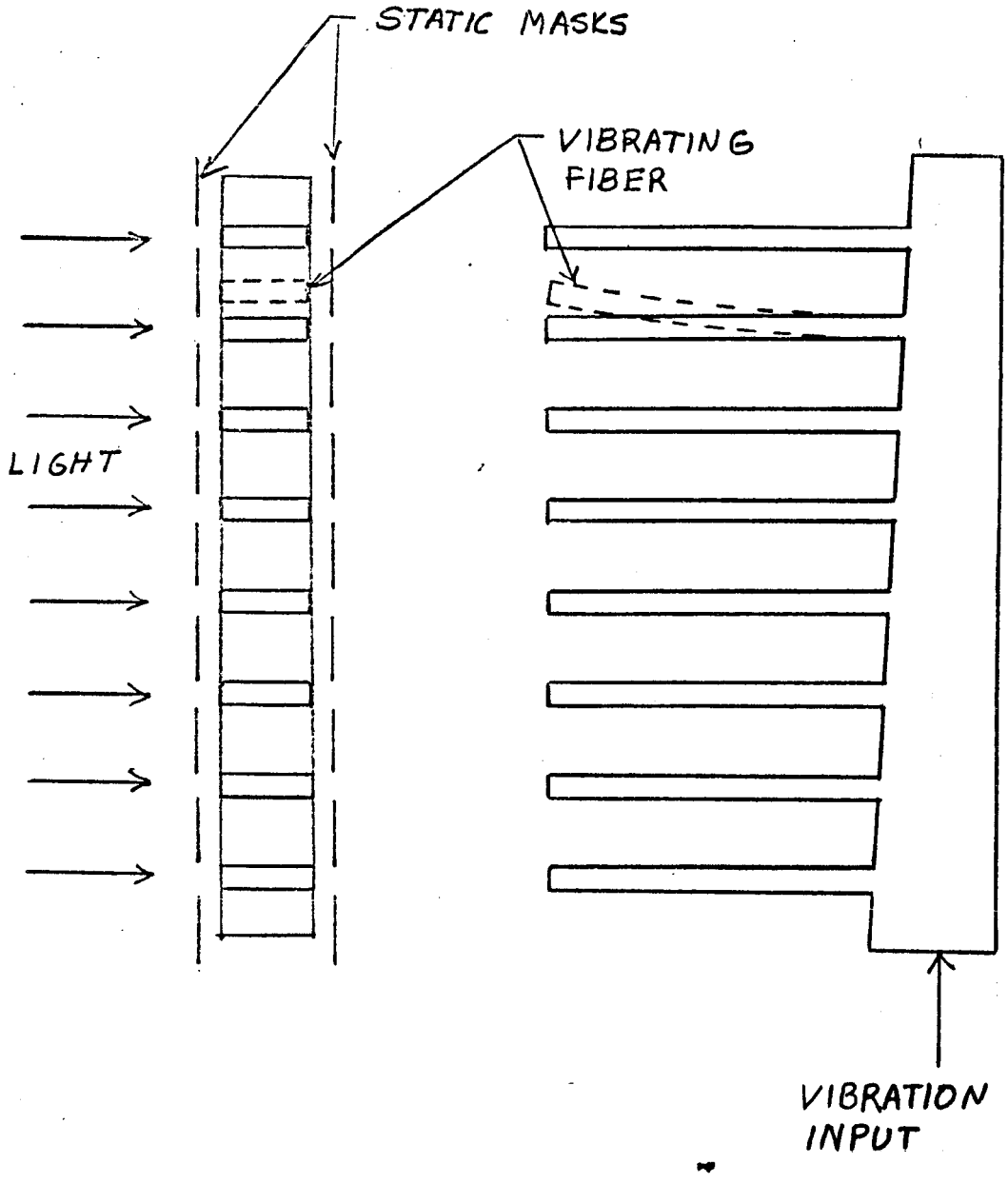

FIGURE 2 - OPERATION OF ARRAY

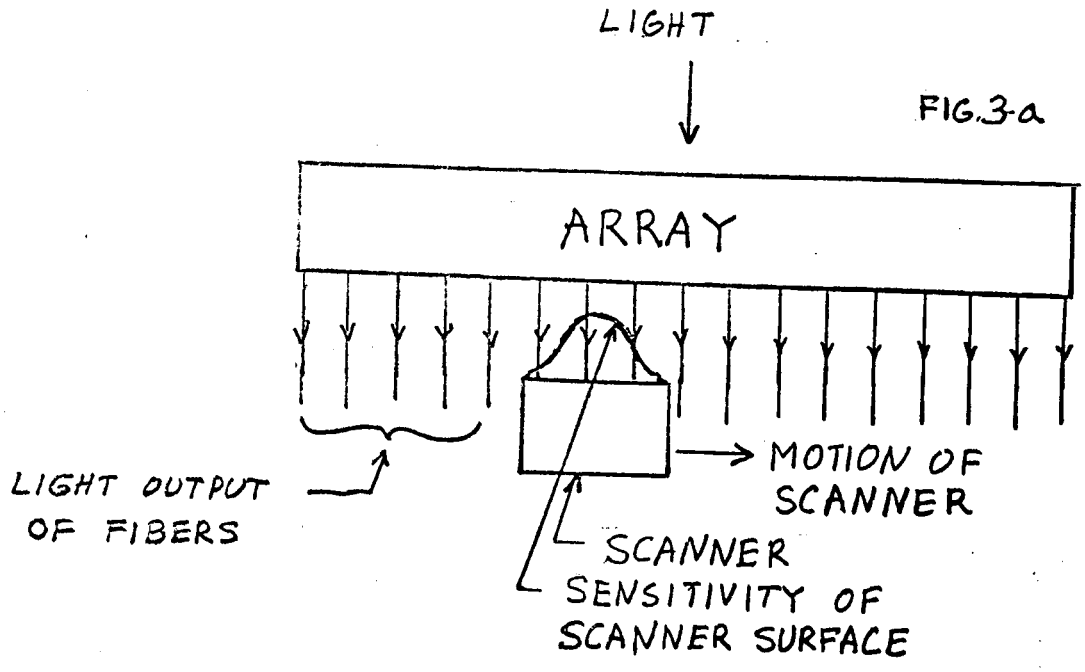

FIG. 3a

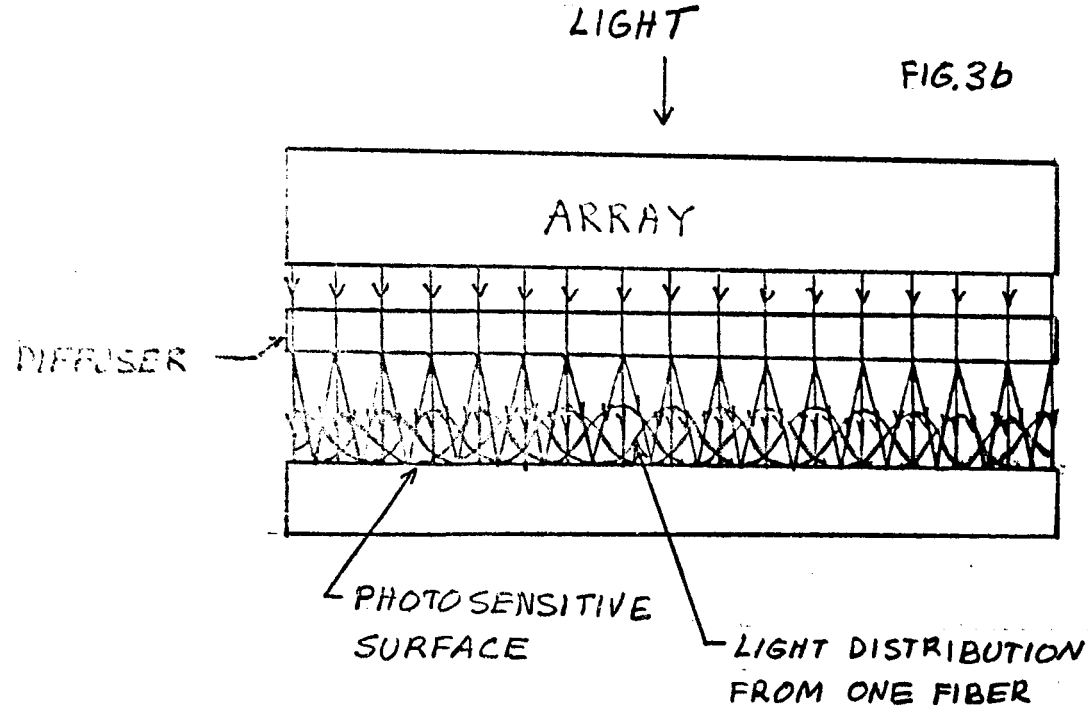

FIG. 3b

FIGURE 3 - TWO METHODS OF SPATIALLY SMOOTHING ARRAY OUTPUT

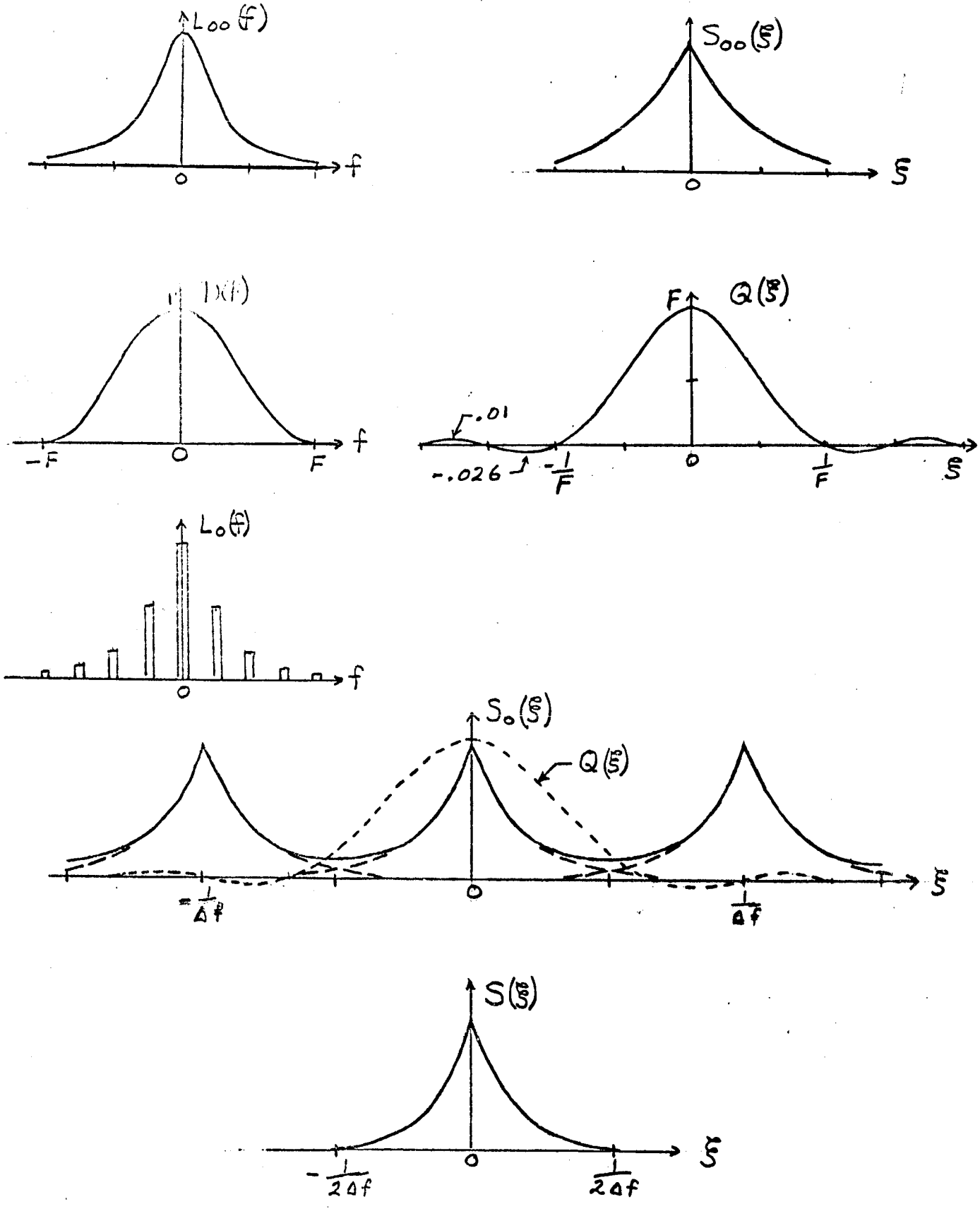

FIGURE 4 - DIFFUSER TREATED AS SPATIAL FILTER

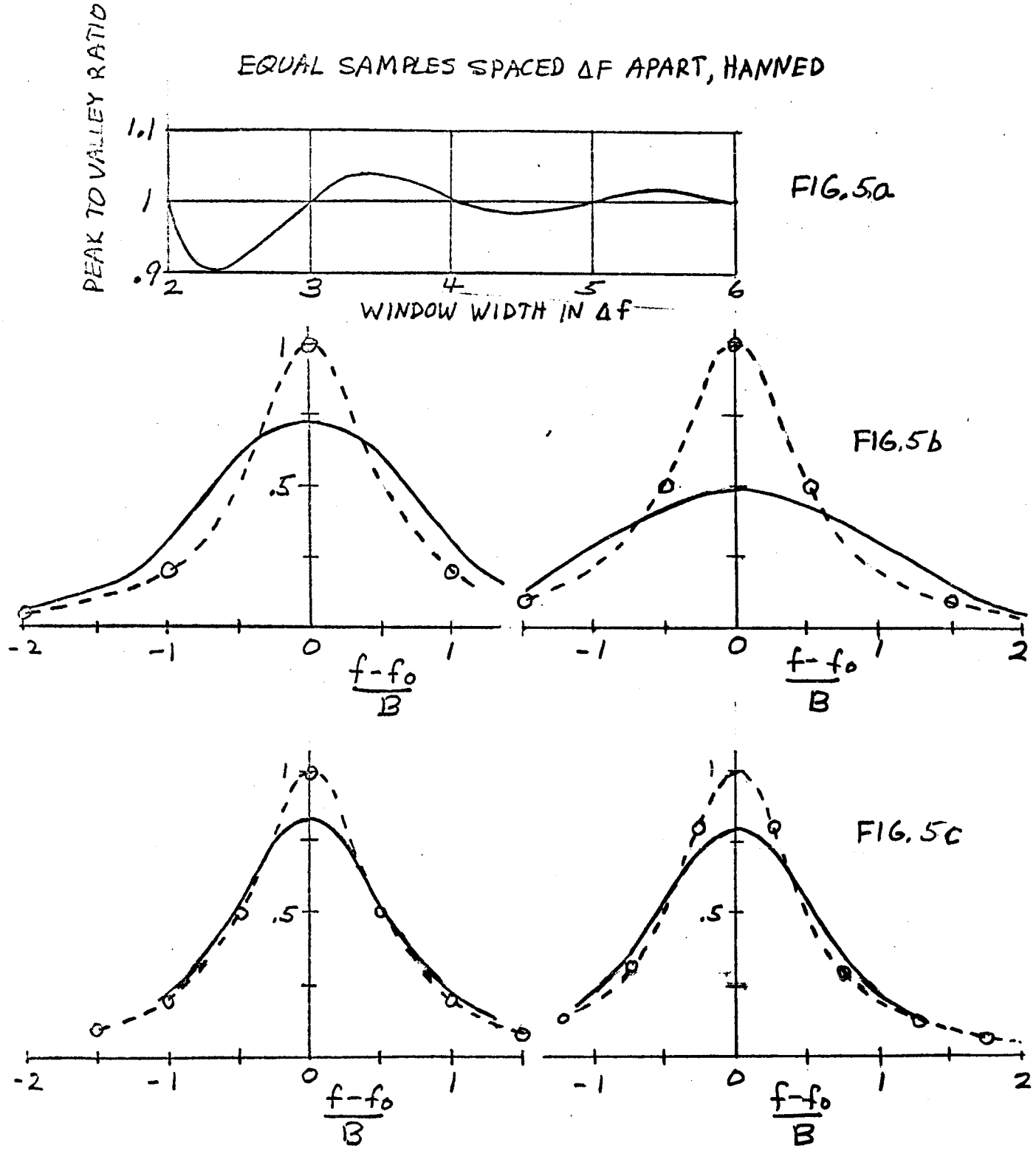

FIGURE 5 - EXAMPLES OF SPATIALLY SMOOTHED ARRAY OUTPUT

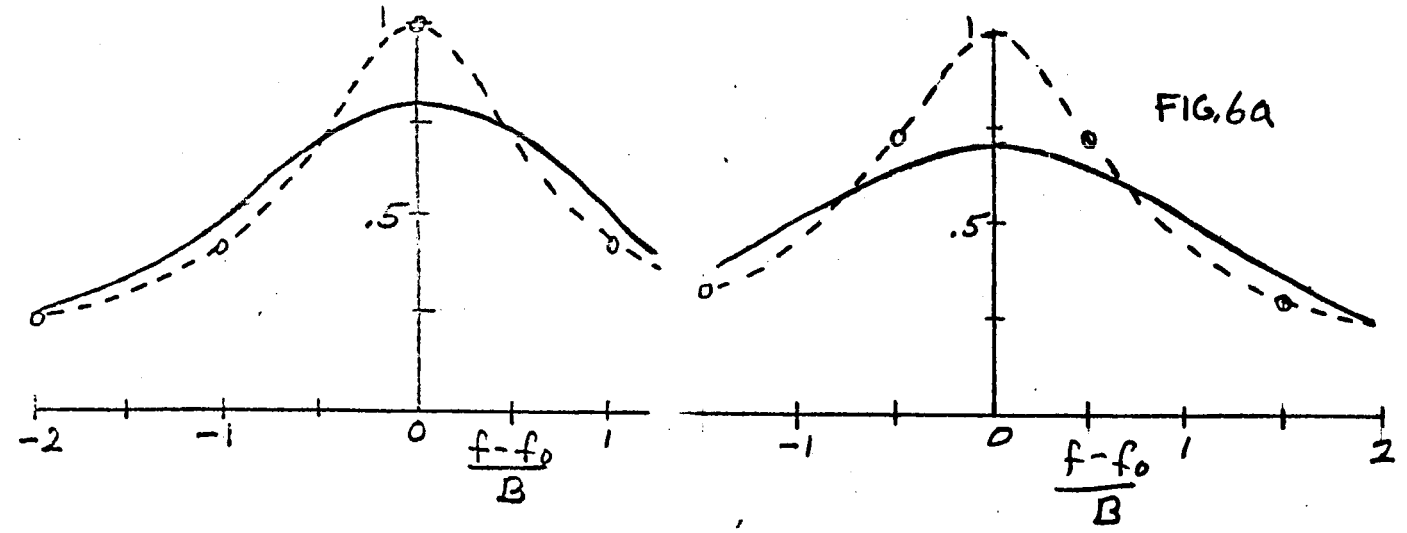

FIG. 6a

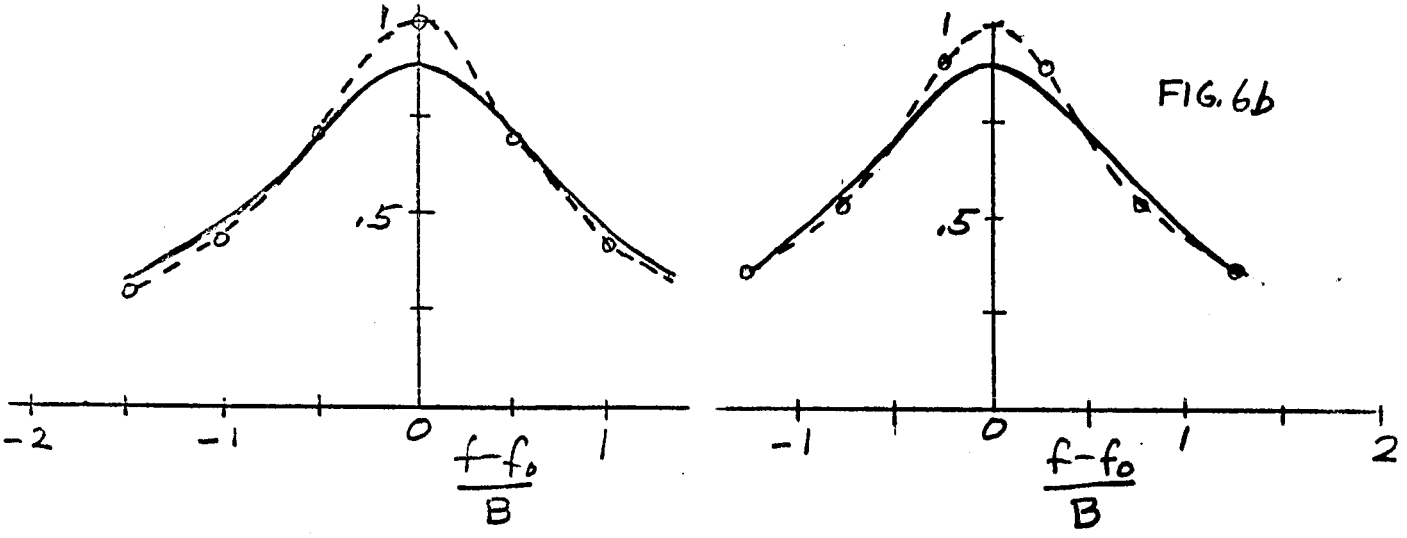

FIG. 6b

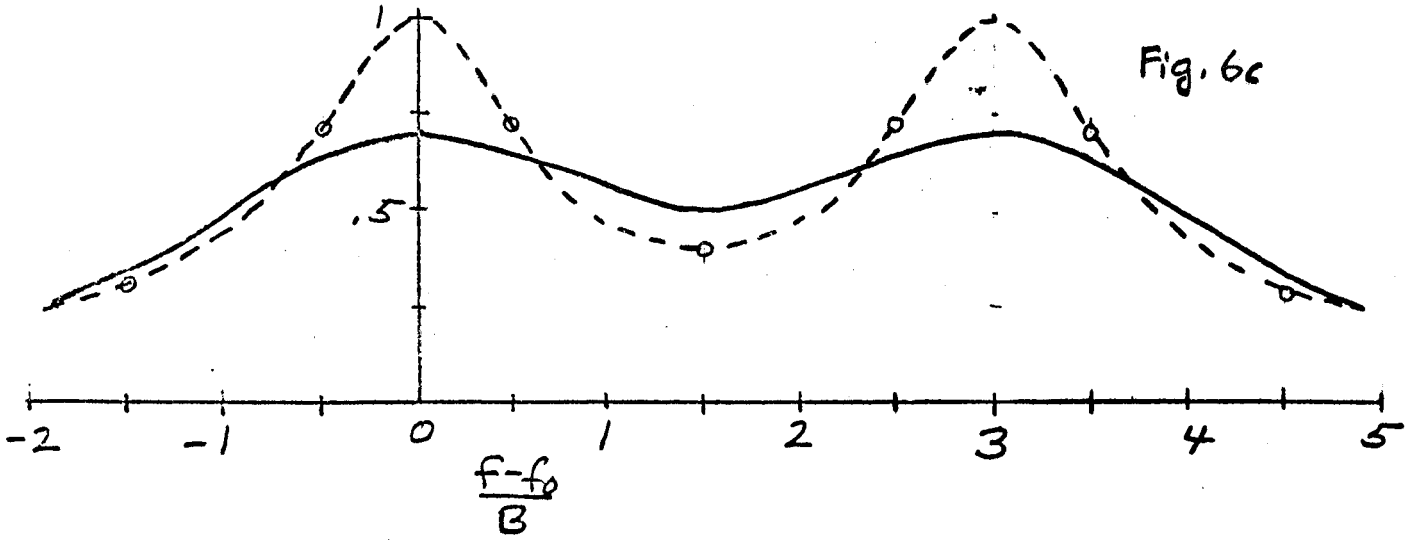

Fig. 6c

FIGURE 6- EXAMPLES OF SPATIALLY SMOOTHED ARRAY OUTPUT

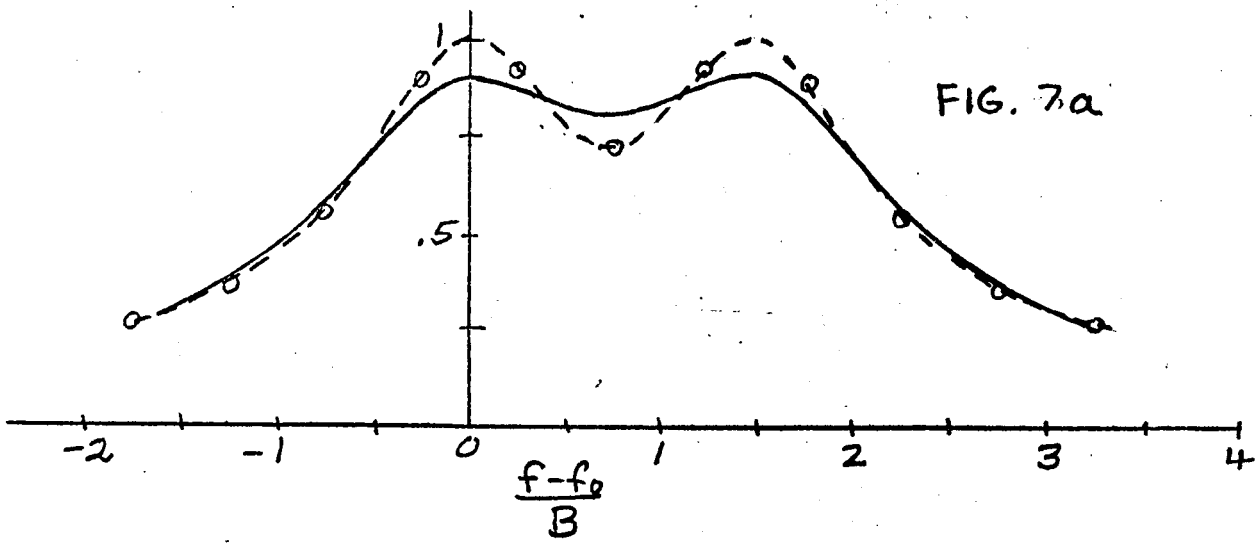

FIG. 7a

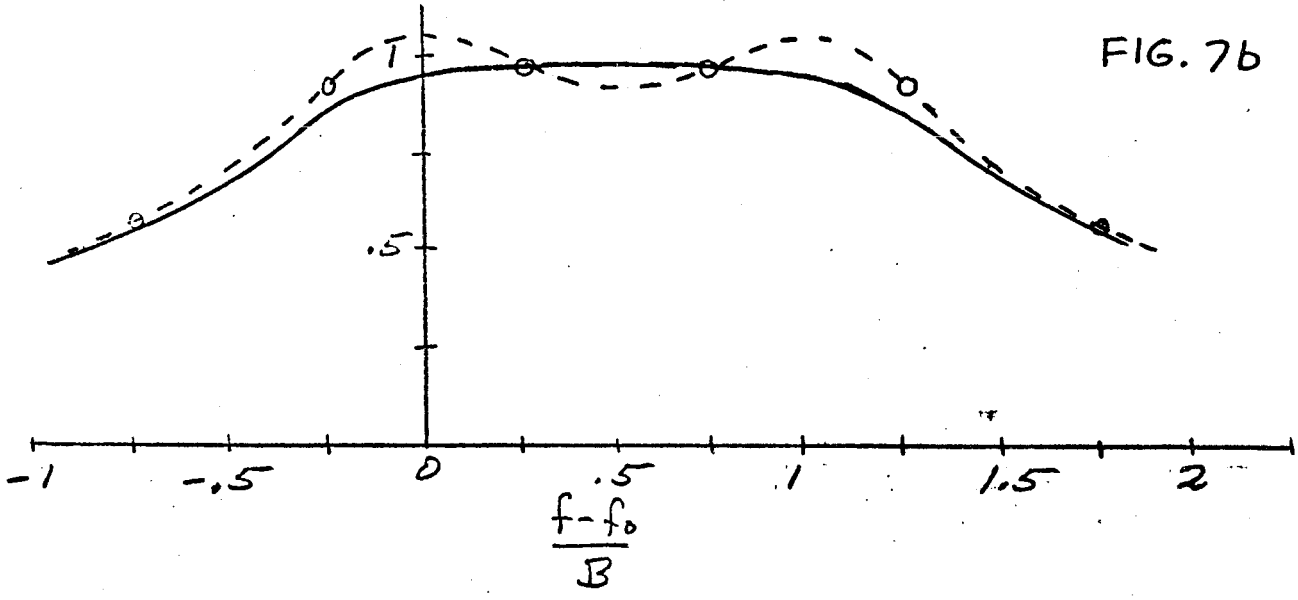

FIG. 7b

FIGURE 7 - EXAMPLES OF SPATIALLY SMOOTHED ARRAY OUTPUT

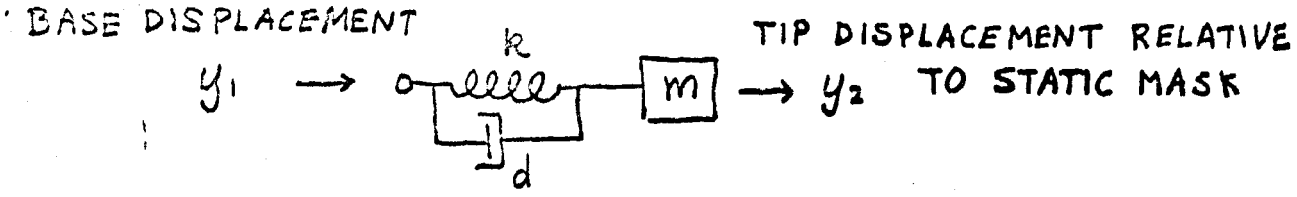

$$\frac{y_2}{y_1} = \frac{-jQ\frac{\omega}{\omega_0}}{1 + jQ\left(\frac{\omega}{\omega_0} - \frac{\omega_0}{\omega}\right)}$$

WHERE $k = \frac{3EI}{\ell^3}$

$m = .226\,\mu\ell$

$\omega_0 = \frac{3.52}{\ell^2}\sqrt{\frac{EI}{\mu}}$

E = MODULUS OF ELASTICITY OF FIBER MATERIAL

I = MOMENT OF INERTIA OF FIBER CROSS SECTION

μ = MASS PER UNIT LENGTH OF FIBER

ℓ = FIBER LENGTH

ω_0 = RESONANT FREQUENCY

Q = Q OF RESONANCE

FIGURE 8- MODEL OF FIBER

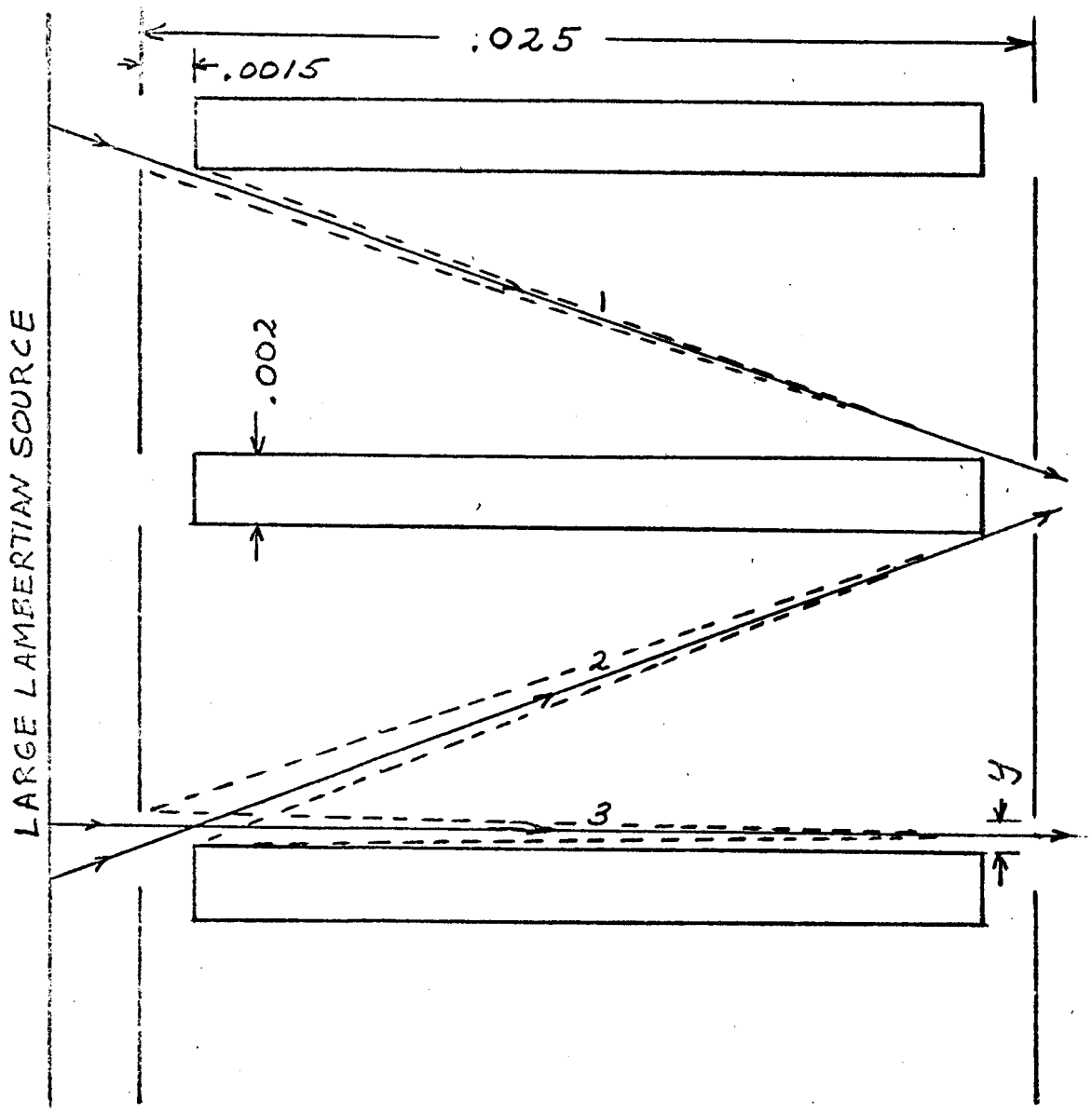

FIGURE 9 - ARRAY ILLUMINATED BY LARGE LAMBERTIAN SOURCE

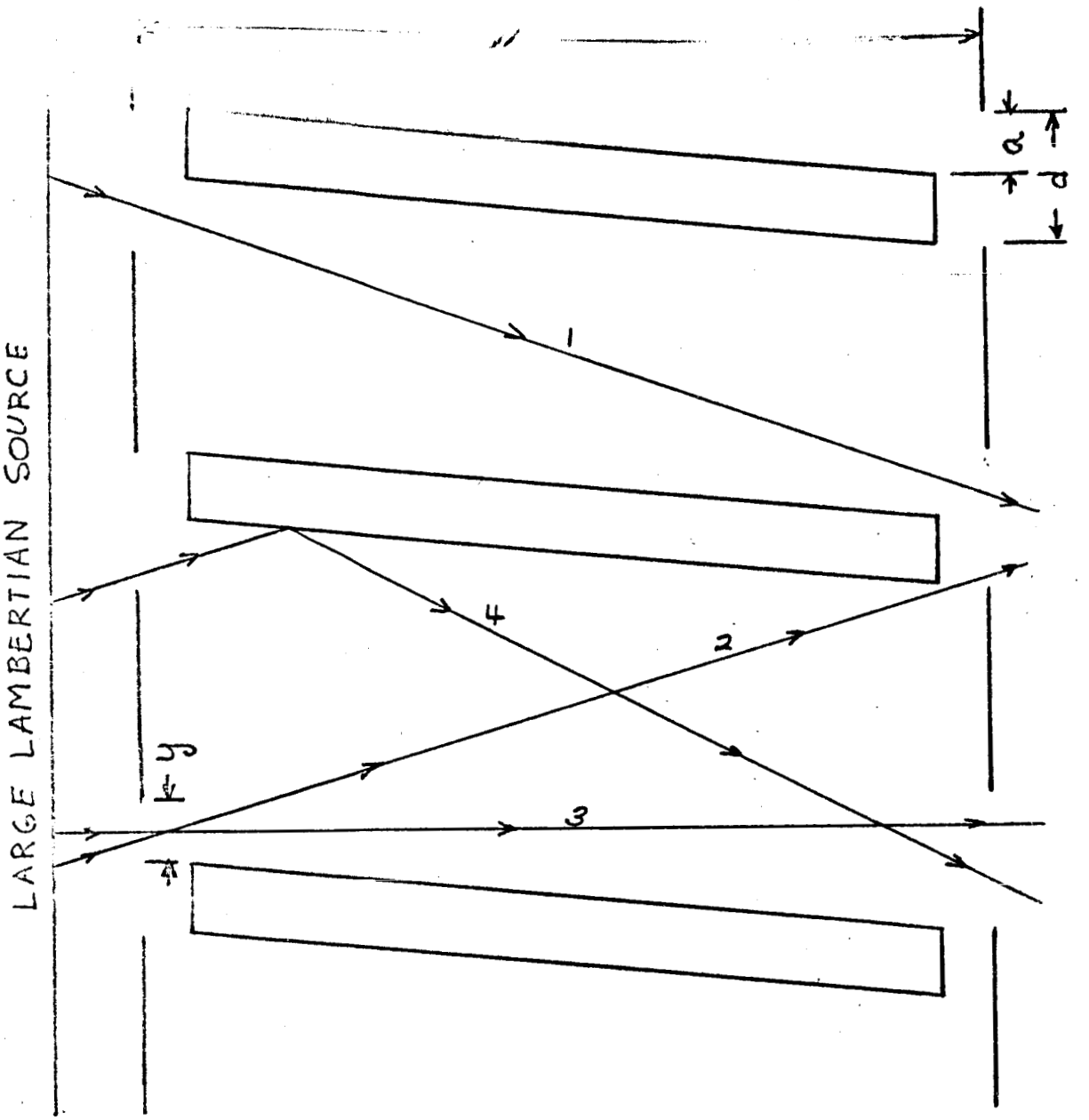

FIGURE 10 - ARRAY ILLUMINATED BY LARGE LAMBERTIAN SOURCE, FIBERS SLANTED

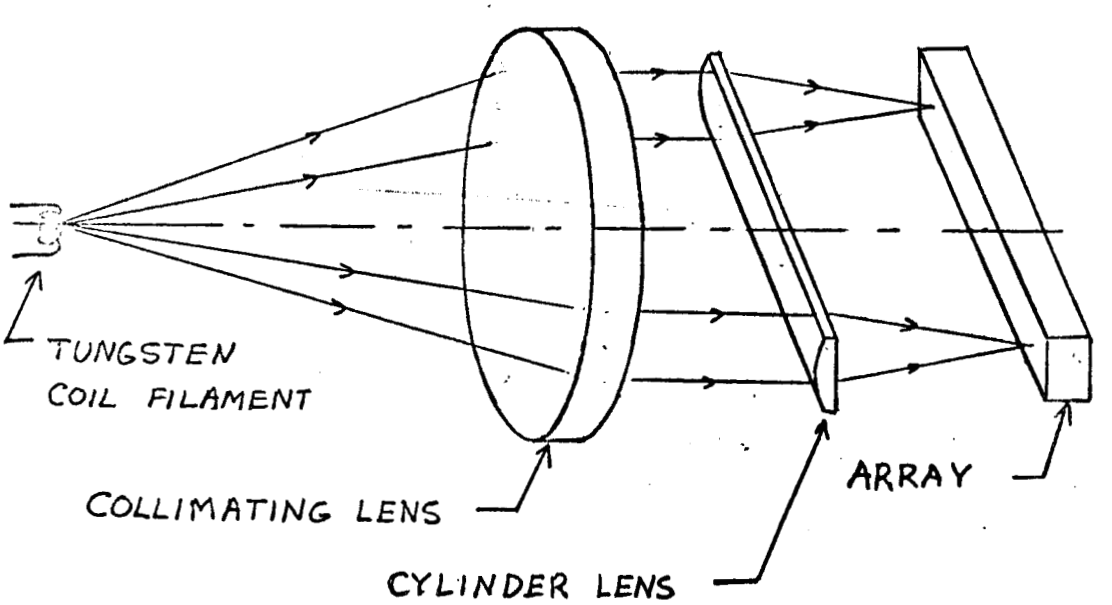

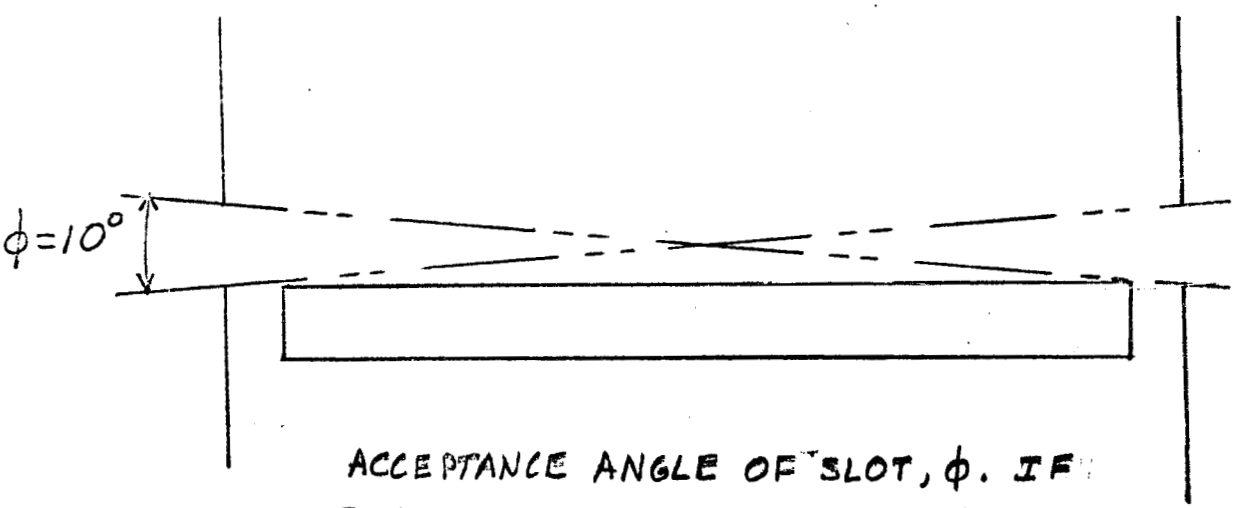

FIGURE 11 - PRACTICAL LIGHT SOURCE

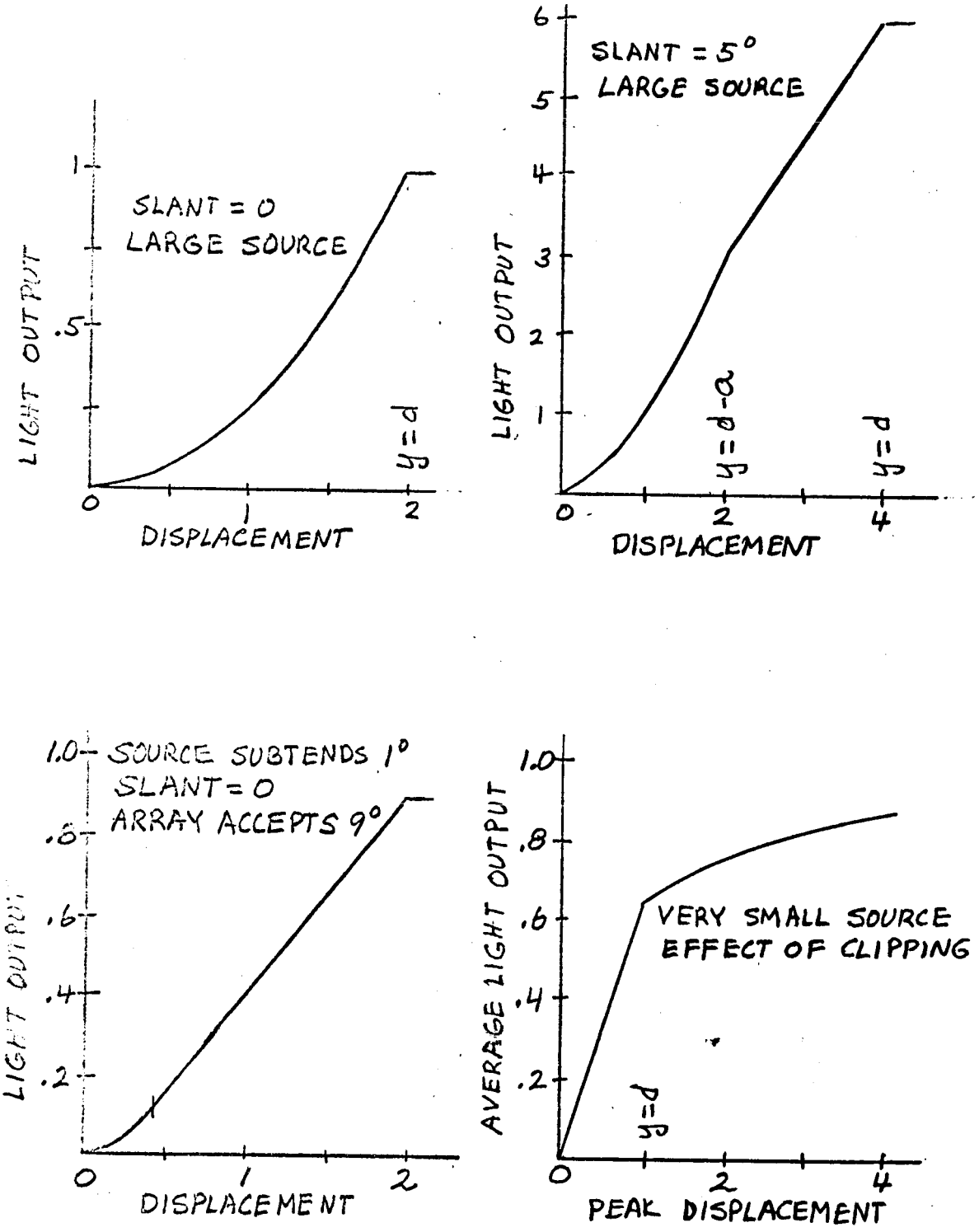

FIGURE 12- FIBER OPTICAL TRANSFER FUNCTION AS FUNCTION OF SOURCE SIZE, FIBER SLANT

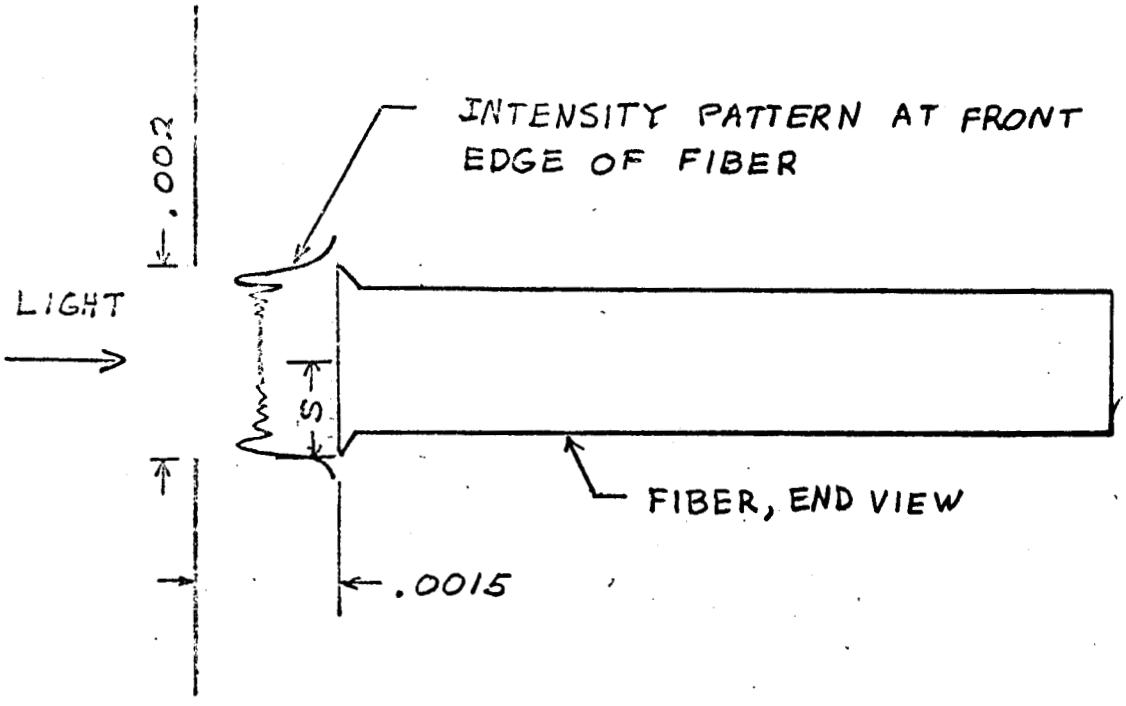

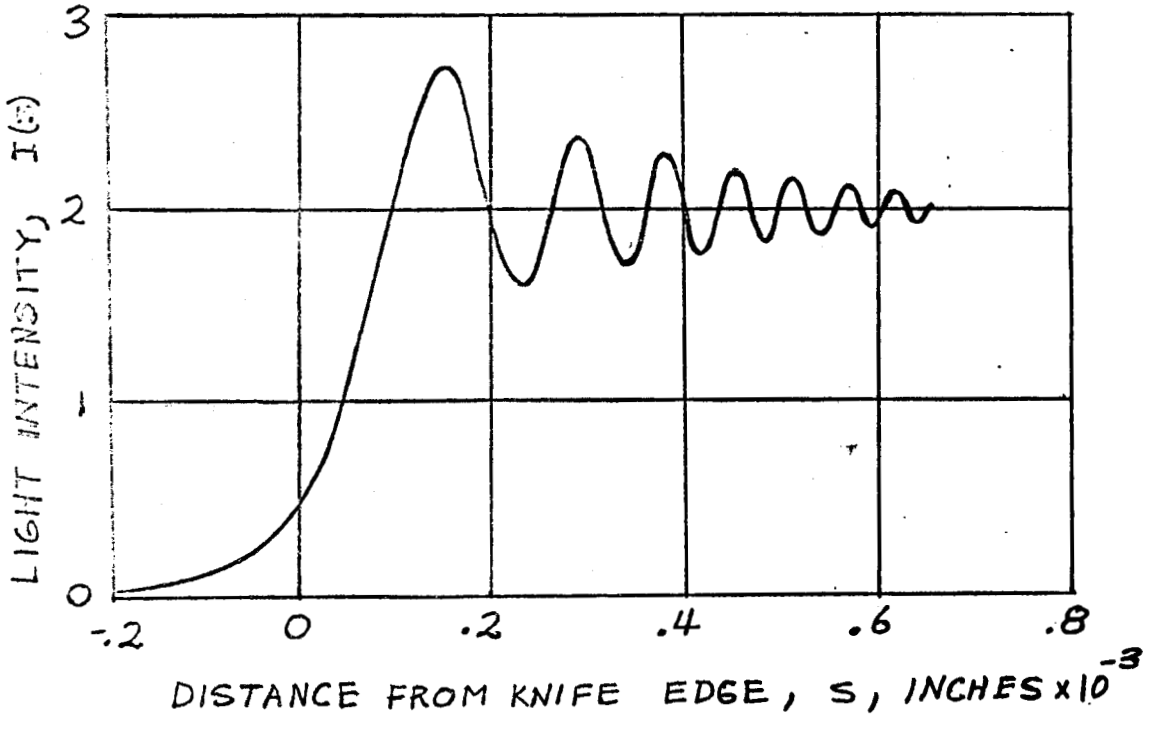

FIGURE 13 - GEOMETRY USED TO CALCULATE DIFFRACTION EFFECTS, MODEL I

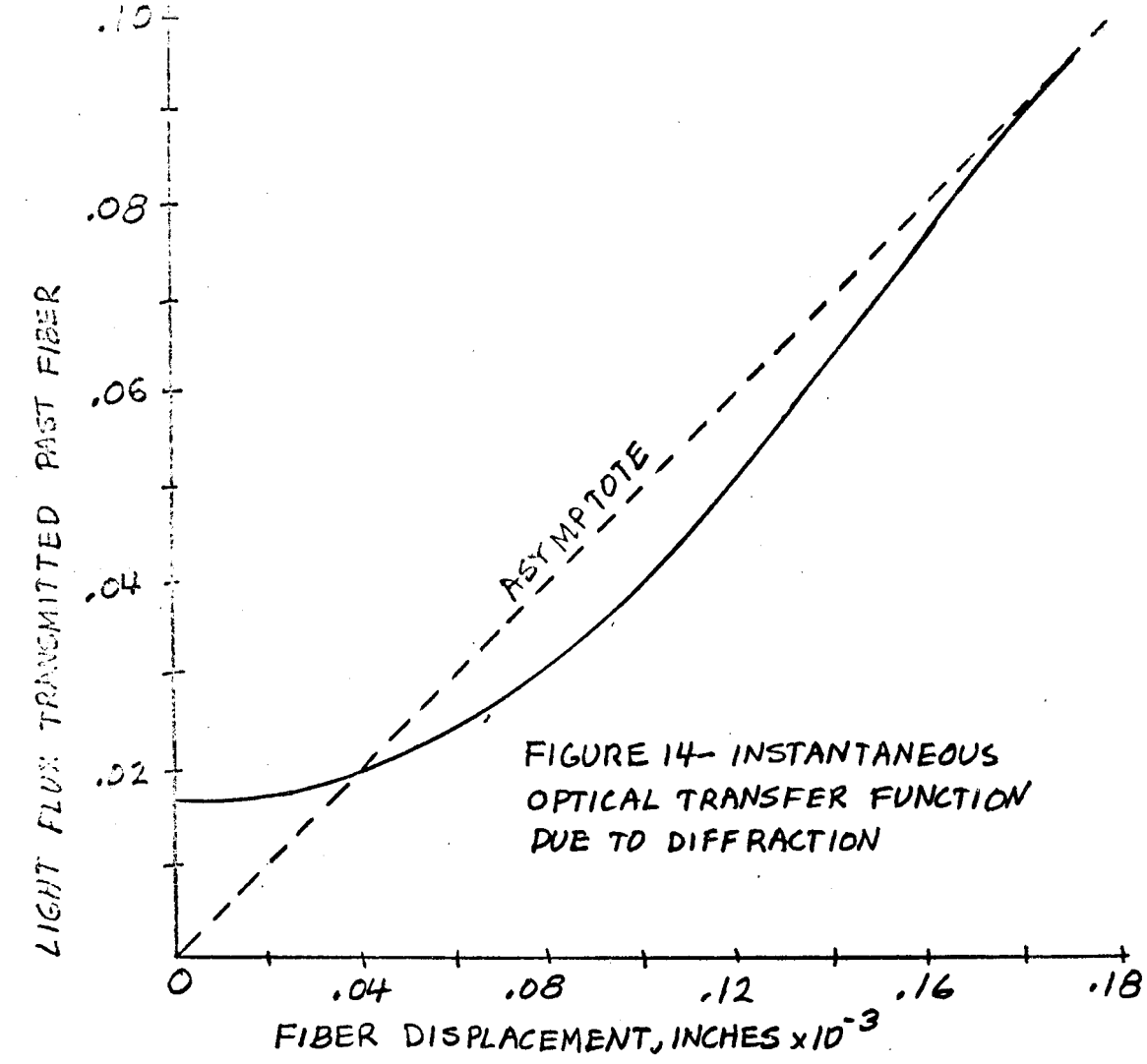

FIGURE 14- INSTANTANEOUS OPTICAL TRANSFER FUNCTION DUE TO DIFFRACTION

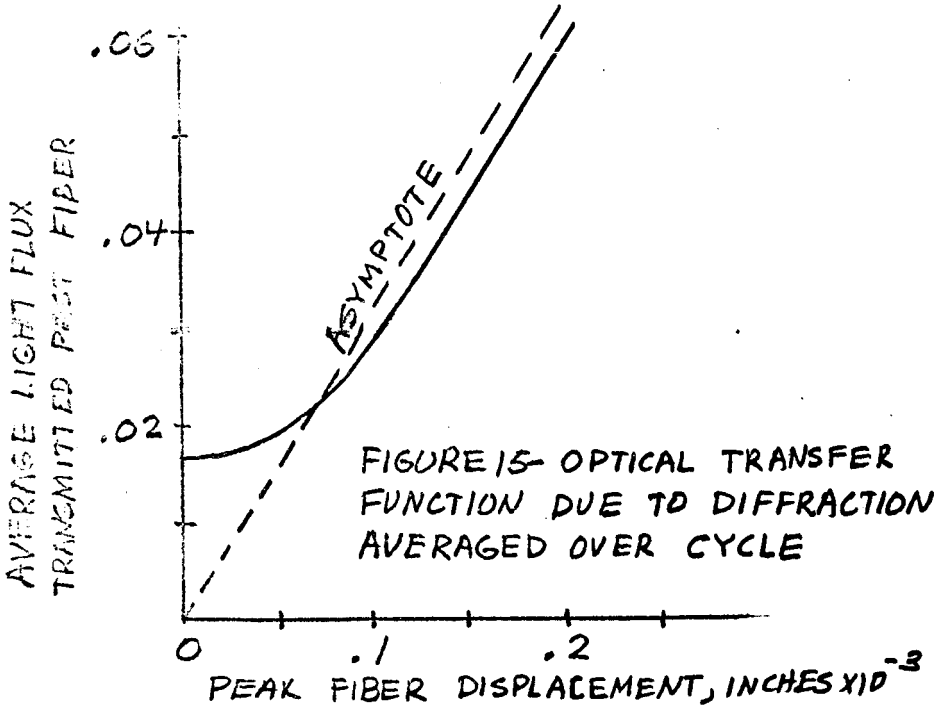

FIGURE 15- OPTICAL TRANSFER FUNCTION DUE TO DIFFRACTION AVERAGED OVER CYCLE

FIG. 16a, MODEL 2

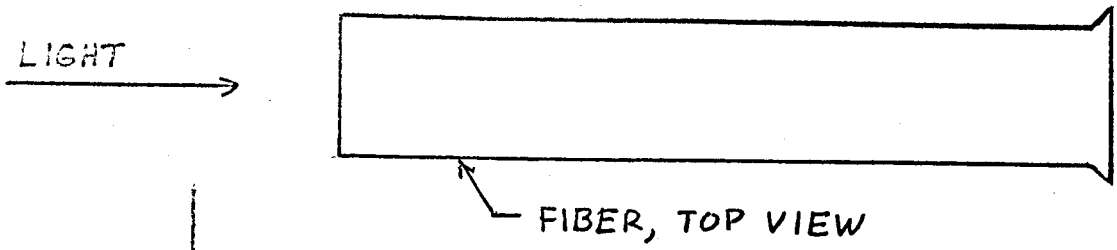

FIG. 16b, MODEL 3

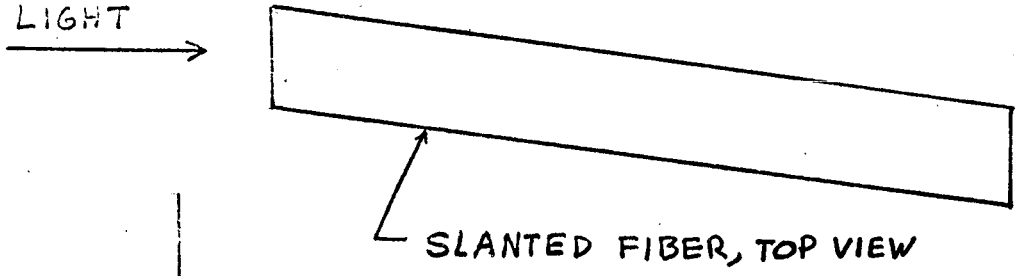

FIGURE 16 – GEOMETRY FOR ESTIMATING DYNAMIC RANGE OF DOUBLE MASK ARRANGEMENT, MODEL 2, 3

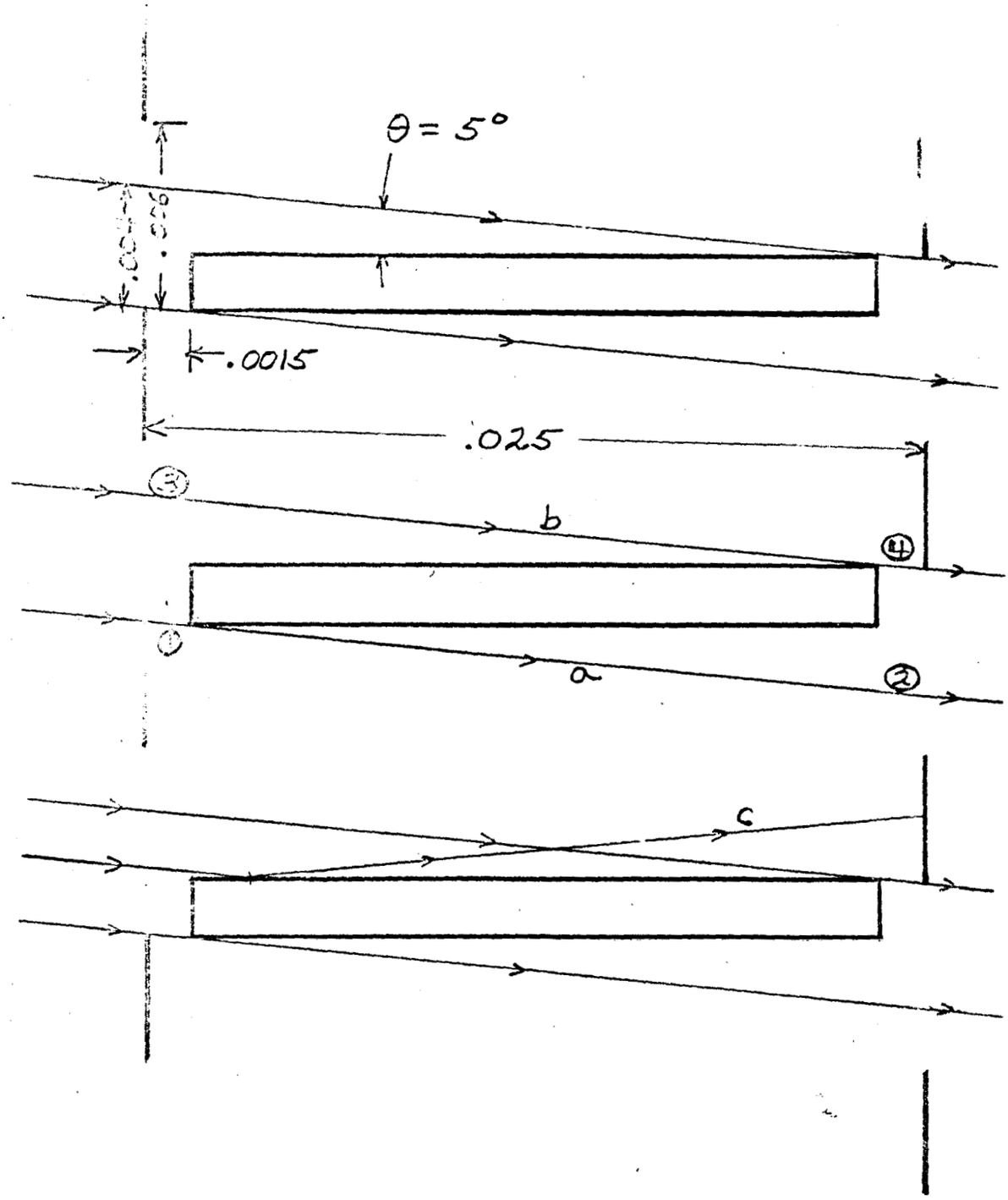

FIGURE 17- DOUBLE MASK GEOMETRY WITH OFFSET SLITS, MODEL 4

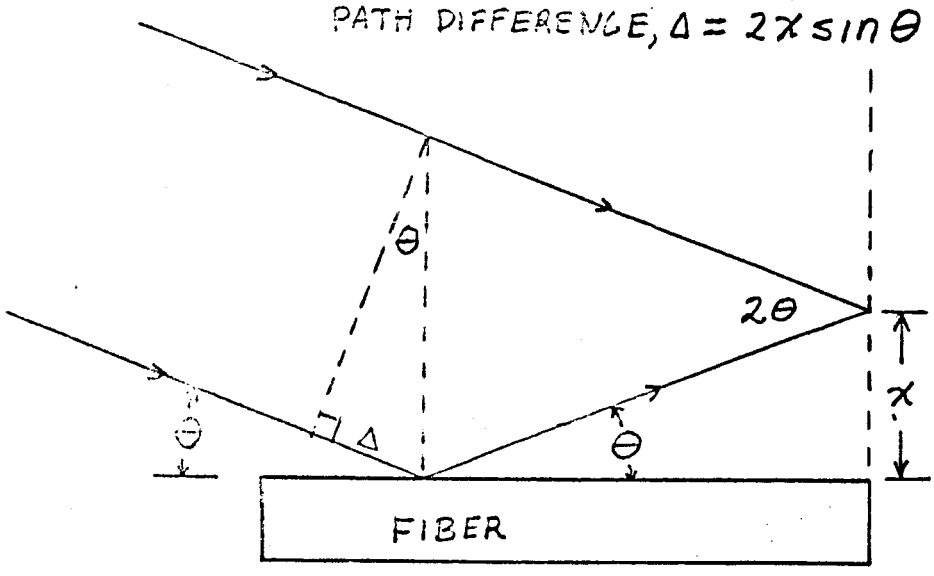

FIGURE 18- INTERFERENCE BETWEEN DIRECT AND REFLECTED WAVES

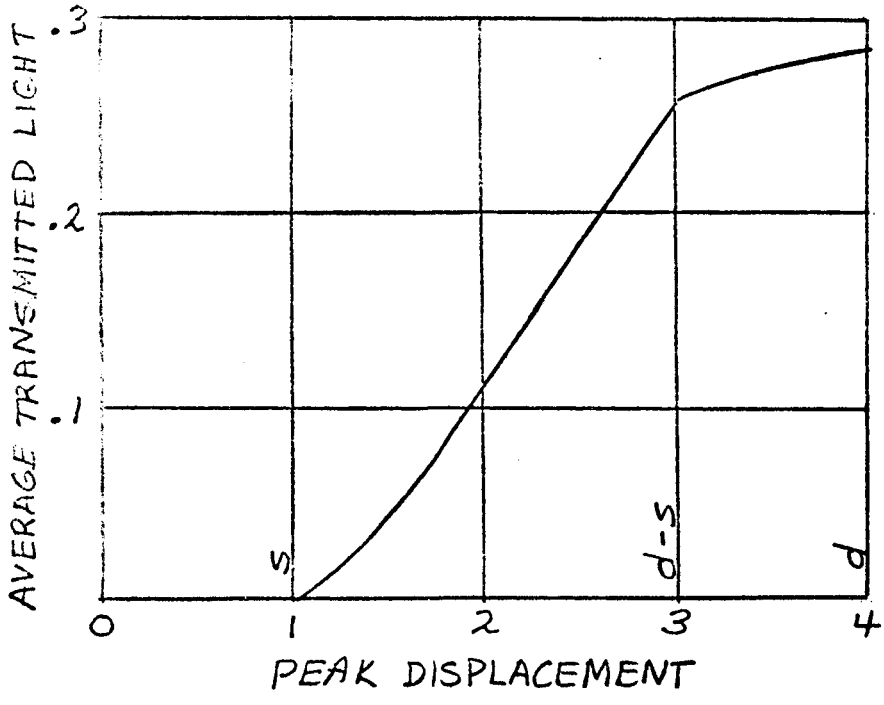

FIGURE 19 - TRANSFER FUNCTION OF DOUBLE MASK WITH BOTH MASKS OFFSET

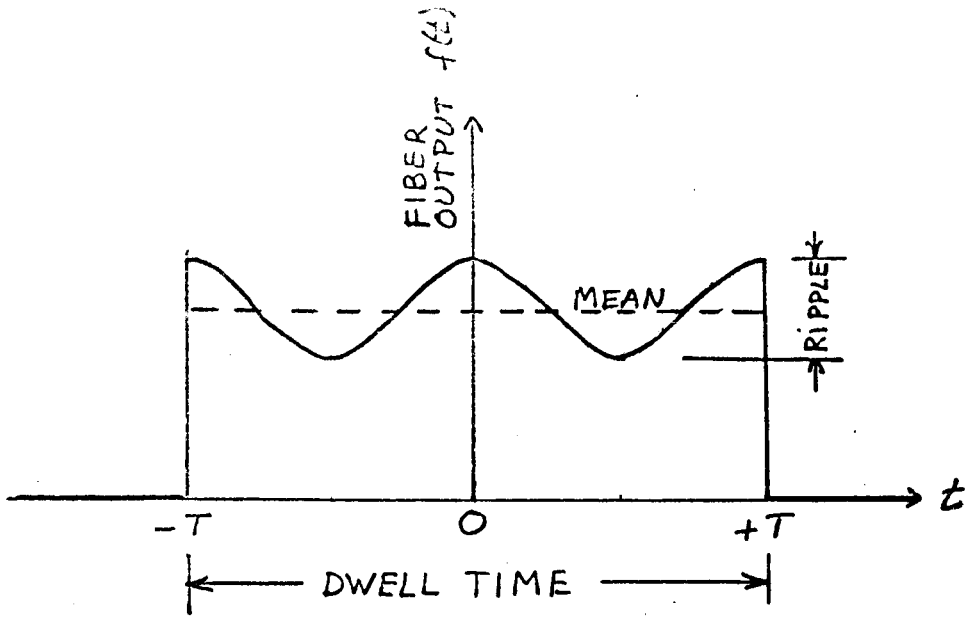

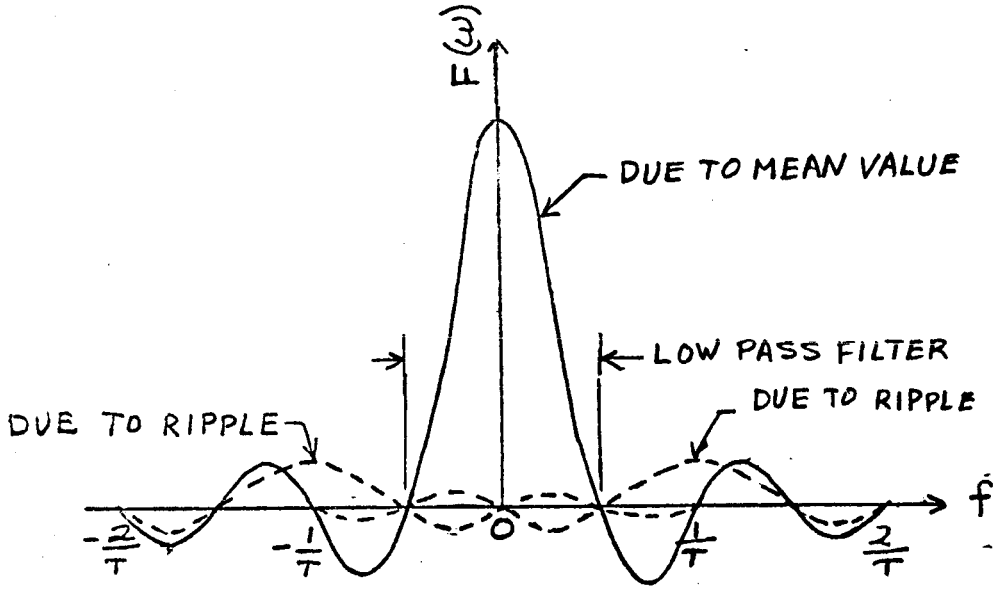

FIGURE 20- SPECTRUM OF SCANNER OUTPUT

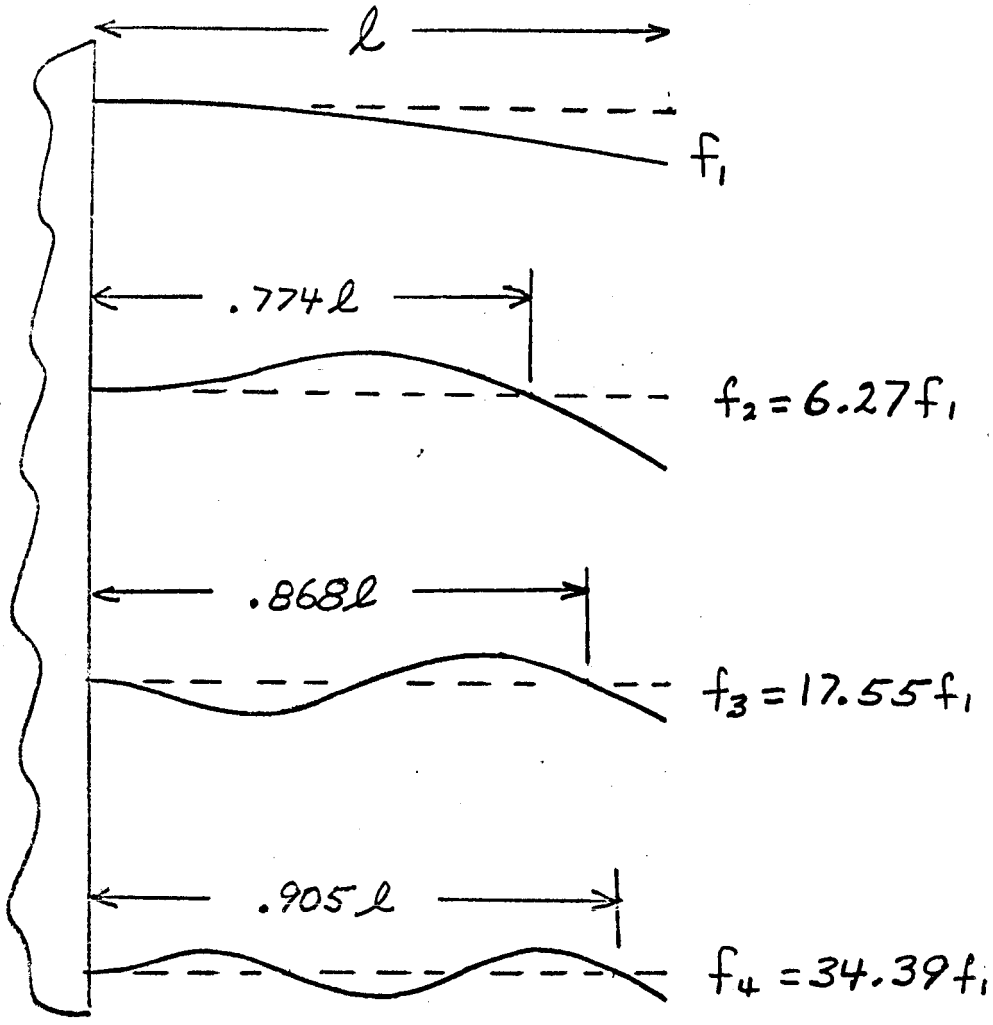

FIGURE 2.1 - HIGHER MODE RESPONSE OF FIBER

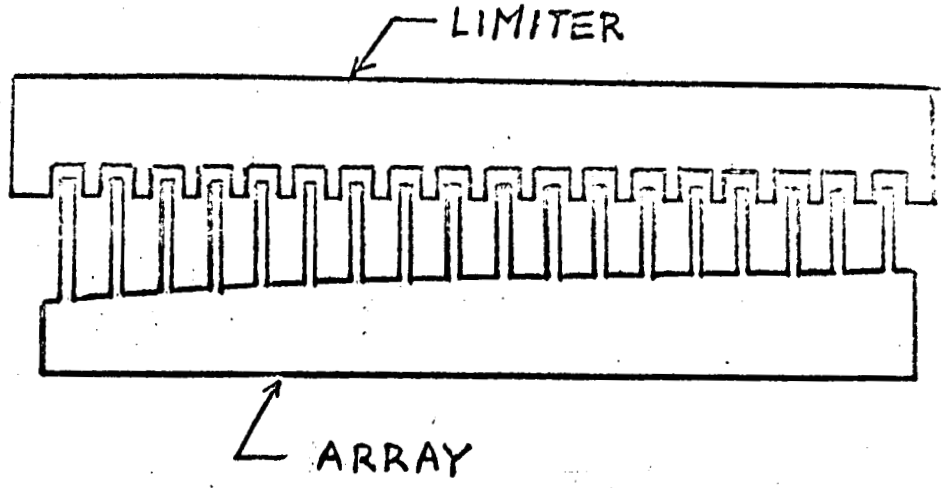

FIGURE 22- FIBER LIMITER

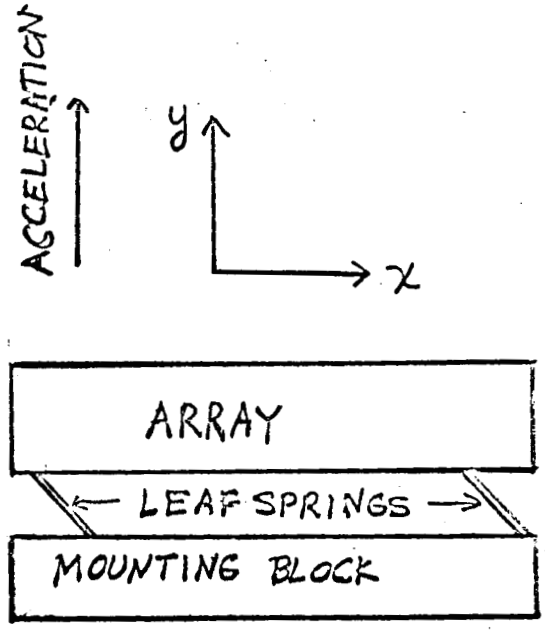

FIGURE 23- MOUNTING WHICH ISOLATES ARRAY FROM STEADY STATE ACCELERATION.

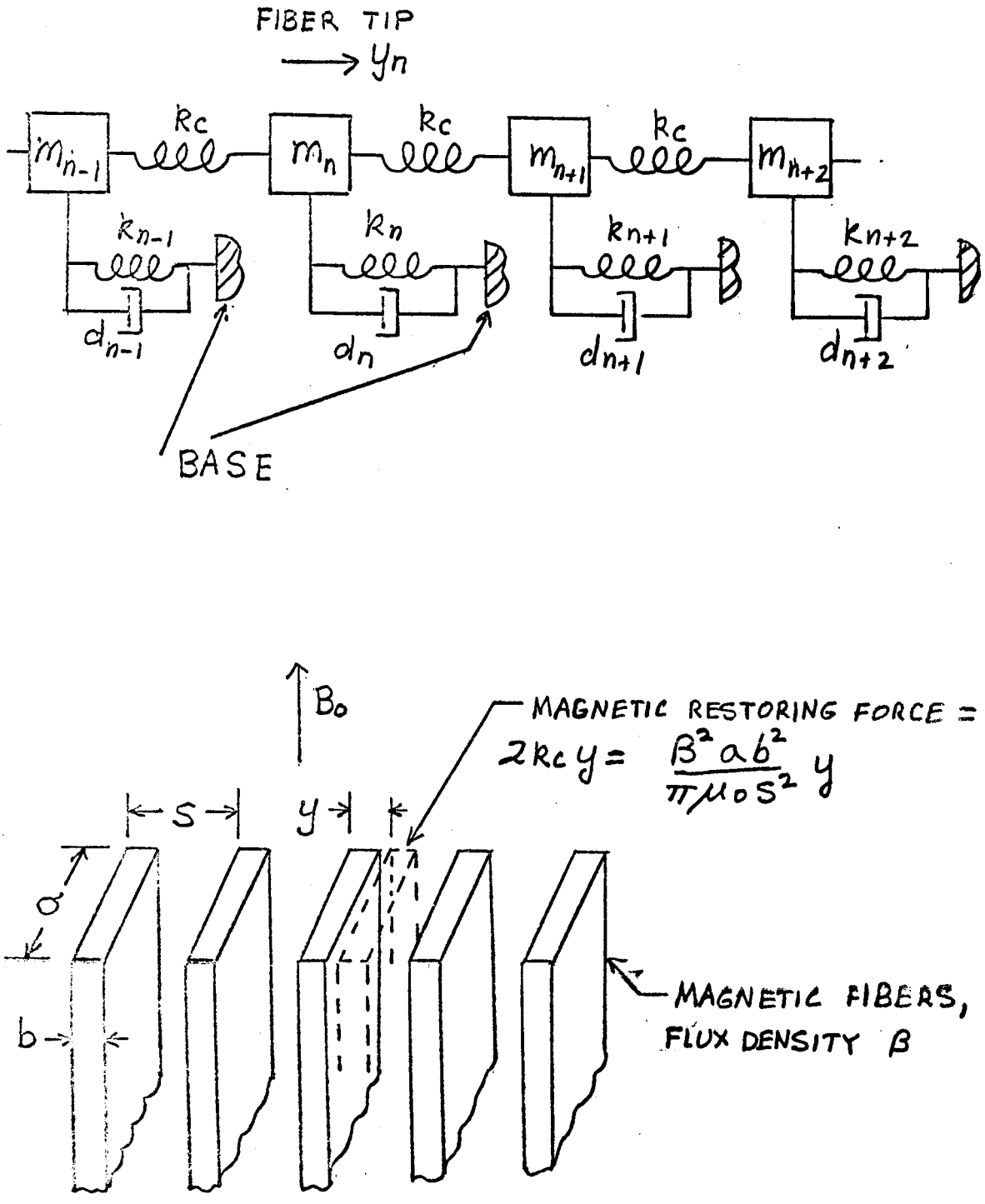

FIGURE 24 - MODEL OF ARRAY WHICH INCLUDES MAGNETIC COUPLING

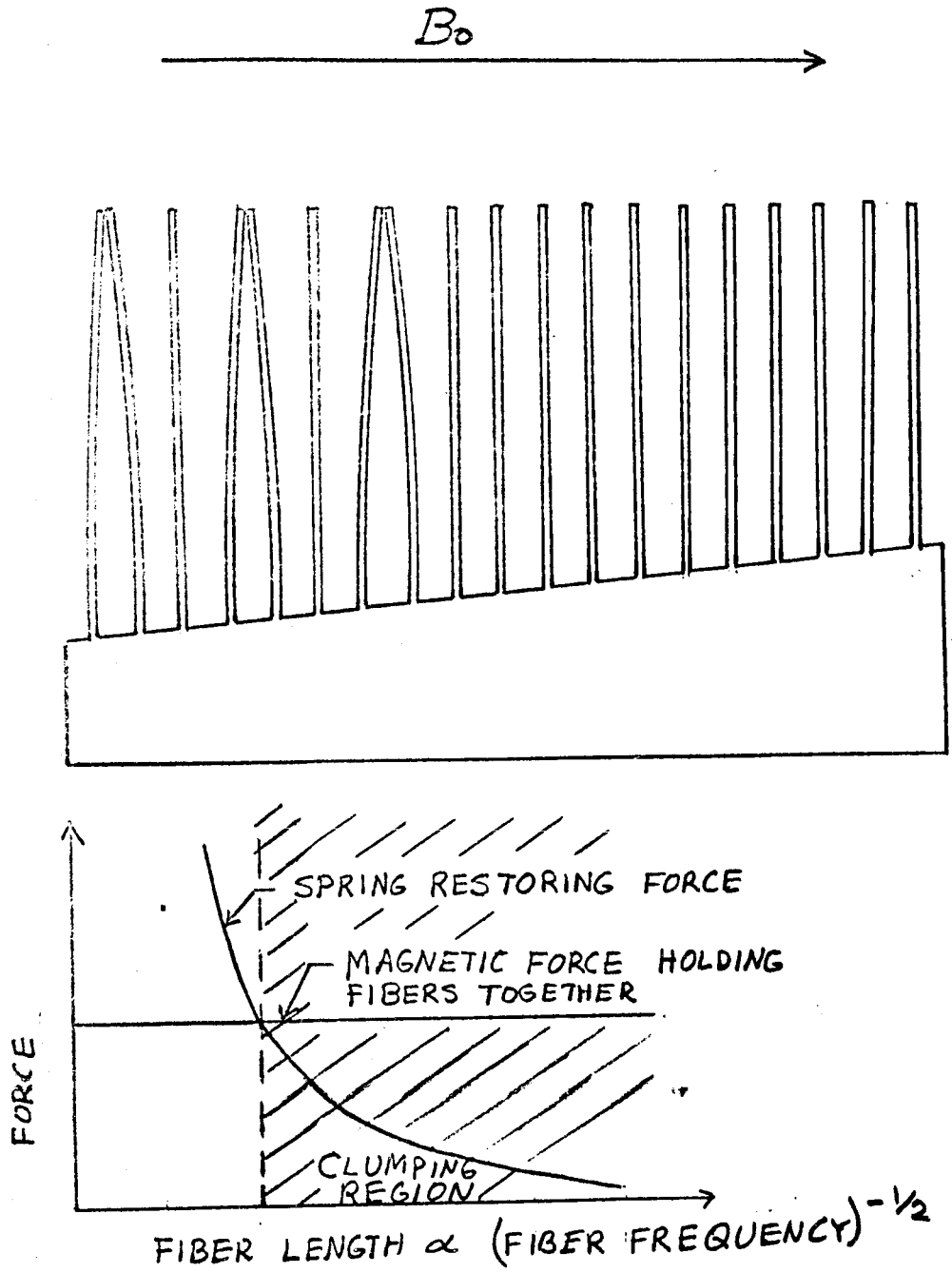

FIGURE 25- FIBER CLUMPING IN TRANSVERSE MAGNETIC FIELD

DISTRIBUTION LIST

Copy No.		Mail Station
1-10	Customer (via J. Higginbotham)	T-214
11	J. Higginbotham	T-214
12	A. Fine	K-37
13	R.S. Hartman	K-37
14	C. Burklund	K-37
15	R. T. Hamlett	1P30
16	Inventions Research	3S118
17	Engineering Library	1A38